Eur. Phys. J. A **30**, 183–202 (2006)
DOI 10.1140/epja/i2006-10116-7

THE EUROPEAN PHYSICAL JOURNAL A

Evolution of the giant dipole resonance properties with excitation energy

D. Santonocito[1,a] and Y. Blumenfeld[2]

[1] INFN - Laboratori Nazionali del Sud, Via S. Sofia 62, I-95123 Catania, Italy
[2] Institut de Physique Nucléaire, IN2P3-CNRS, F-91406 Orsay, France

Received: 7 March 2006 /
Published online: 31 October 2006 –

Abstract. The studies of the evolution of the hot Giant Dipole Resonance (GDR) properties as a function of excitation energy are reviewed. The discussion will mainly focus on the $A \sim 100$–120 mass region where a large amount of data concerning the width and the strength evolution with excitation energy are available. Models proposed to interpret the main features and trends of the experimental results will be presented and compared to the available data in order to extract a coherent scenario on the limits of the development of the collective motion in nuclei at high excitation energy. Experimental results on the GDR built in hot nuclei in the mass region $A \sim 60$–70 will be also shown, allowing to investigate the mass dependence of the main GDR features. The comparison between limiting excitation energies for the collective motion and critical excitation energies extracted from caloric curve studies will suggest a possible link between the disappearance of collective motion and the liquid-gas phase transition.

PACS. 24.30.Cz Giant resonances – 25.70.Ef Resonances – 25.70.Gh Compound nucleus

1 Introduction

A well-established result of nuclear physics is the observation of giant resonances, small amplitude, high frequency, collective modes of excitation in nuclei. Among all possible modes of collective excitation, the Giant Dipole Resonance (GDR), a collective vibration of protons against neutrons with a dipole spatial pattern, has been widely investigated and is now considered a general feature of all nuclei.

The experiments performed over many years have shown that the GDR is an efficient tool to probe nuclear properties of the ground state as well as at finite temperature. In fact, the gamma-ray emission due to the GDR decay is sufficiently fast to compete with other decay modes with a sizable branching ratio and therefore to probe the characteristics of the nuclear system prevailing at that time. The resonance energy being proportional to the inverse of the nuclear radius, the investigation of the strength distribution gives access to the study of the nuclear deformations in the ground state but also to the shape evolution of nuclei as a function of spin and temperature of the system. Shape evolution and shape fluctuations are the main issues in the study of the GDR in nuclei populated at low excitation energy ($E^* < 100\,\mathrm{MeV}$) and spin up to the fission limit. This region has been extensively studied and the GDR properties, which are expected to be influenced by shell effects, are rather well understood [1,2] even if some recent results indicate an interesting discrepancy between data and theoretical models at temperatures $T \sim 1$–$1.5\,\mathrm{MeV}$ which deserves further investigation.

Conversely, populating nuclei at progressively higher thermal energies up to the limits of their existence, one can follow the evolution of the collective motion in extreme conditions up to its disappearance. The investigation of the GDR features at high excitation energy is particularly interesting because it also opens up the possibility to investigate the limits of validity of the standard statistical scenario in describing the decay properties of hot nuclei. The statistical model assumes, in fact, that the system reaches thermal equilibrium before it decays. Increasing the excitation energy, the compound nucleus lifetime decreases significantly and collective degrees of freedom might not reach equilibrium before the system decays. Therefore, the GDR strength distribution will reflect the relative influence of the different time scales which come into play, the population and decay time of the GDR on one hand and the equilibration and decay times of hot nuclei on the other. In the following the experimental results collected up to $E^* \sim 500\,\mathrm{MeV}$ will be presented and compared to statistical model calculations. The evidence in the gamma spectra of a vanishing of the GDR strength at high excitation energies relative to the standard statis-

[a] e-mail: santonocito@lns.infn.it

tical calculation led to the development of different theoretical models whose main features will be discussed in the text. The comparison between data and statistical calculations including different model prescriptions will allow us to draw some conclusions concerning the effects leading to the GDR disappearance. Eventually, the existence of a limiting excitation energy for the collective motion will be discussed and compared to the limiting excitation energies extracted from the caloric-curve studies in different mass regions. This will allow to investigate a link between the liquid-gas phase transition and the disappearance of collective motion.

2 GDR built on the ground state: general features

The GDR was first observed in 1947 by Baldwin and Klaiber in photo-absorption and photo-fission experiments [3,4]. They observed an increase of the absorption cross-section above 10 MeV in several nuclei with resonance energies between 16 and 30 MeV.

The observed peak in the photo-absorption spectrum was interpreted by Goldhaber and Teller [5] as the excitation of a collective nuclear vibration in which all the protons in the nucleus move collectively against all the neutrons creating an electric dipole moment. Since then, the GDR has been extensively studied, and a broad systematics for almost all stable nuclei exists on the GDR built on ground states. Most of the information was extracted from photo-absorption experiments because of the high selectivity of this reaction to $E1$ transitions [6].

The shape of the resonance in the photo-absorption spectrum can be approximated, in the case of a spherical nucleus, by a single Lorentzian distribution [6,7]:

$$\sigma_{abs}(E_\gamma) = \frac{\sigma_0 E_\gamma^2 \Gamma_{GDR}^2}{(E_\gamma^2 - E_{GDR}^2)^2 + E_\gamma^2 \Gamma_{GDR}^2}, \qquad (1)$$

where σ_0, E_{GDR} and Γ are, respectively, the strength, the centroid energy and the width of the Giant Dipole Resonance. In nuclei with a static deformation, the GDR splits in two components corresponding to oscillations along and perpendicular to the symmetry axis, and the cross-section for photo-absorption can be well reproduced by the superposition of two Lorentzian distributions. This particular feature allows one to extract the nuclear deformation from the centroid energies of the two components and to distinguish, from the relative intensities, prolate from oblate deformations.

The systematics shows that the resonance energy decreases gradually with increasing mass number. This mass dependence can be reproduced by [6]:

$$E_{GDR} = 31.2A^{-1/3} + 20.6A^{-1/6} \qquad (2)$$

which is a linear combination of the mass dependencies predicted by Goldhaber-Teller and Steinwedel-Jensen macroscopic models for the energy of the GDR [5,7].

The width of the resonance is also strongly influenced by the shell structure of the nuclei. The systematics shows values ranging from about 4–5 MeV for closed-shell nuclei up to about 8 MeV for nuclei between closed shells [6].

The collectivity of the excitation, which is related to the number of participating nucleons, can be estimated in terms of the Energy-Weighted Sum Rule (EWSR) for dipole radiation. This sum rule, also known as Thomas-Reiche-Kuhn (TRK) sum rule gives the total integrated cross-section for electric dipole photon absorption. It is given by:

$$\int_0^\infty \sigma_{abs}(E_\gamma)\mathrm{d}E_\gamma = \frac{2\pi^2 e^2 \hbar}{Mc}\frac{NZ}{A} = 60\frac{NZ}{A}(\mathrm{MeV}\cdot\mathrm{mb}), \qquad (3)$$

where N, Z and A are, respectively, the neutron, the proton and the mass number and M is the nucleon mass [6]. The systematics shows that for nuclei of mass $A < 80$ the TRK sum rule is not exhausted by the data while in the region of mass $A \sim 100$ the photoneutron cross-section integrated up to about 30 MeV exhausts the TKR sum rule [6]. For heavier mass nuclei the experimental data exceed the TKR sum rule by about 20–30% [6].

3 GDR built on excited states: historical

The field of the study of Giant Resonances built on excited states was launched by Brink [8] who stated the hypothesis that Giant Resonances could be built on all nuclear states and that their characteristics, aside from the dependence on the shape, should not depend significantly on the nuclear state. This opened up the possibility of investigating nuclear shapes also in excited nuclei and to study the evolution of the properties of collective motion up to the limits of existence of nuclei. Indeed the disappearance of collective motion has been considered a further signature for a phase transition in nuclear matter.

Evidence in favor of the Brink hypothesis was extracted for the first time in 1974, in the study of the γ-ray spectrum emitted from spontaneous fission of ^{252}Cf [9]. The enhancement observed in the γ spectrum above 10 MeV was, in fact, correctly attributed to the de-excitation of the GDR built on excited states of the fission products. The first evidence for the existence of the GDR built on an excited state using a reaction study emerged in a proton capture (p,γ) experiment on ^{11}B where the GDR built on the first excited state of ^{12}C was observed [10]. From subsequent (p,γ) and (n,γ) experiments on various other light nuclei emerged a coherent picture supporting the Brink hypothesis [11]. An important step further in the study of the GDR properties was made with the use of heavy-ion reactions which opened up the possibility to populate highly excited continuum states through the mechanism of complete fusion in a wide variety of nuclei. The first observation of the gamma-decay of the GDR built on highly excited states in nuclei formed in fusion

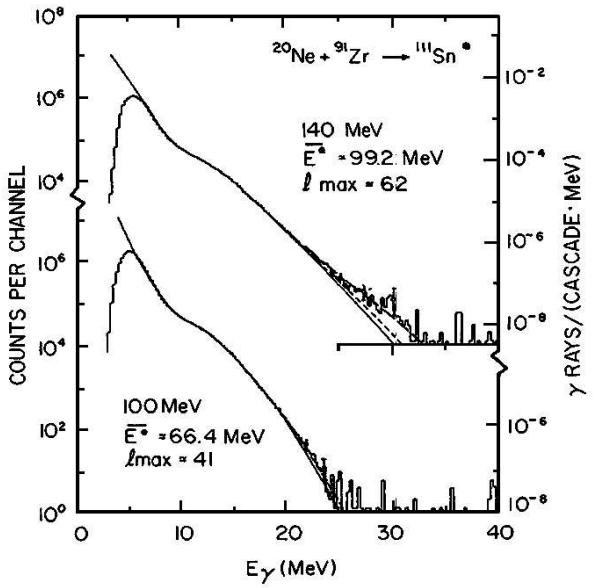

Fig. 1. Measured γ-ray spectra from the decay of ^{111}Sn at $E^* = 66$ and $E^* = 100$ MeV. Full lines represent the statistical-model calculations using a level density parameter $a = A/8$ while the short-dashed line is a similar calculation with $a = A/8.5$ and the long-dashed one is obtained including the decay from the giant quadrupole resonance [24].

reaction was made in 1981 studying ^{40}Ar-induced reactions on ^{82}Se, ^{110}Pd, and ^{124}Sn targets [12]. The importance of these measurements stems from the fact that they demonstrated the possibility to study the GDR in the γ-ray de-excitation spectra following fusion reactions where the statistical emission of high-energy gamma-rays occurs from an equilibrated system and in competition with particle evaporation indicating a sizable branching for gamma decay. The experiments performed since then have been focused on establishing the existence of the GDR built on excited states as a general feature of nuclei and on the evolution of the parameters governing the GDR properties as a function of the excitation energy, spin and mass.

4 GDR built on excited states: general features

When the GDR built on excited states is studied at increasing excitation energy the scenario becomes gradually more complex due to the opening of different decay channels. In heavy-ion collisions up to 5–6A MeV the reaction dynamics are dominated by mean-field effects which lead, for central collisions, to a complete fusion of projectile and target nuclei. In this case a compound nucleus is formed with a well-defined excitation energy and a broad distribution in angular momentum. The equilibrated system will then undergo a statistical decay emitting light particles and gamma-rays according to their relative probabilities which can be very well accounted for in the framework of the statistical model. Gamma-rays can be emitted at all steps during the decay sequence and the emission of a high-energy gamma-ray will be in competition with light-particle emission, driven by the ratio of the level densities between initial and final states for both decay channels. In general light-particle emission is much more probable than γ-decay, but the latter, which has a probability of the order of 10^{-3}, is a more useful probe of the GDR properties since the γ-ray carries all the energy of the resonance. The decay rate R_γ is given by

$$R_\gamma \mathrm{d}E_\gamma = \frac{\rho(E_2)}{\hbar\rho(E_1)} f_{GDR}(E_\gamma)\mathrm{d}E_\gamma \,, \tag{4}$$

where $\rho(E_1)$ and $\rho(E_2)$ are, respectively, the level densities for the initial and final states which differ by an energy $E_\gamma = E_1 - E_2$ and $f_{GDR}(E_\gamma) \propto \sigma_{abs} E_\gamma^2$. It can be written as

$$f_{GDR}(E_\gamma) = \frac{4e^2}{3\pi\hbar mc^3} S_{GDR} \frac{NZ}{A} \times \frac{\Gamma_{GDR} E_\gamma^4}{(E_\gamma^2 - E_{GDR}^2)^2 + E_\gamma^2 \Gamma_{GDR}^2} \,, \tag{5}$$

where σ_{abs} is the photo-absorption cross-section and S_{GDR} is the fraction of the exhausted sum rule. Comparing the above expressions with the neutron emission rate it follows that the GDR gamma yield is higher during the first steps of the decay cascade [1]. This means that, if the decay is statistical, the GDR γ-rays essentially reflect the GDR properties at the highest excitation energies. Besides, since the nuclear level density varies exponentially with the excitation energy the number of transition photons decreases exponentially with transition energy. This last argument together with the competition at all steps in the emission process reflects and explains the shape of the measured gamma-ray spectrum. A typical spectrum measured studying the decay of the GDR in hot nuclei populated in complete-fusion reactions between heavy ions at beam energies up to 5–6A MeV is shown in fig. 1. Below $E_\gamma \sim 10$ MeV the spectrum is dominated by the statistical emission of gamma-rays from the equilibrated system at the end of the decay process. Above $E_\gamma \sim 10$ MeV a broad bump is observed which is a signature of the GDR decay.

In order to extract quantitative information on the GDR properties at different excitation energies from the spectrum we need to make a comparison with statistical calculations which take into account all the decay sequence. This kind of analysis is usually carried out using the statistical code CASCADE [13] which treats the statistical emission of neutrons, protons, alphas and γ-rays from a hot equilibrated system. In the code, the GDR is assumed to be Lorentzian in shape in analogy to the observation made on cold nuclei. The dipole emission is expected to dominate the spectrum above 10–12 MeV even if small contributions from quadrupole emission cannot be ruled out and are typically included in the calculation. All the results strongly depend on the assumptions made for the level densities.

In the following, the results concerning the GDR properties will be discussed for increasing excitation energy. We will generally assume that E^* and T can be related by the Fermi-gas formula $E^* = aT^2$ [14]. An extensive discussion of the determination of the level density parameter a can be found in ref. [15]. The main part of the discussion will be focused on mass region $A \sim 120$ due to the existing broad systematics. The discussion will be divided in two main sections, one for experiments up to $E^* \sim 200$ MeV where the main issue is the increase of the GDR width while the strength retains its full collective character and a second one, above $E^* \sim 200$ where a progressive quenching of the GDR, is observed in all the experiments. A detailed analysis of this effect will be undertaken from the theoretical and the experimental point of view leading to some conclusions concerning the GDR properties up to the limits of its existence.

5 The evolution of the GDR at moderate excitation energies up to 200 MeV

Once the main features of GDR built on the ground state are well understood the question arises as to what happens to GDR properties built on the excited states. In this case the main aim is to probe the stability of collective motion in nuclei under increasing temperature and angular momentum. In particular, populating hot nuclei at increasing excitation energy and in different spin ranges one is able to follow the shape modifications and fluctuations associated to the weakening of shell effects which dominate the nuclear properties of the ground state. At the same time it is also possible to extract new information on the relative time scales involved in shape rearrangements. A further important issue in these studies is the evaluation of the relative influence of angular momentum and temperature effects on the evolution of the GDR parameters. In a typical fusion experiment the higher excitation energies are associated to large transfer of angular momentum. Recently, inelastic scattering has been used to populate nuclei in a wide range of excitation energies with little angular momentum transfer allowing to disentangle the relative contribution of angular momentum and temperature effect on the GDR features.

The existing hot GDR systematics can be reasonably well accounted for in the framework of the adiabatic thermal fluctuation model [16–19]. However, recent results on width measurements in the region of temperatures below about 1.5 MeV showed important discrepancies between predictions and data in different mass regions which remain hitherto unexplained [19–22]. In the following, we will concentrate on tin isotopes ($A \sim 110$) tracing an historically based overview of our understanding of the GDR features up to now. In this mass region the GDR built on the ground state is characterized by a resonance energy of about 15 MeV, a strength fulfilling 100% of the EWSR and a width of about 5 MeV. A significant modification of the GDR width was observed for the first time by Gaardhøje *et al.* [23] studying the gamma spectra emitted in the statistical decay of ^{108}Sn nuclei populated up to

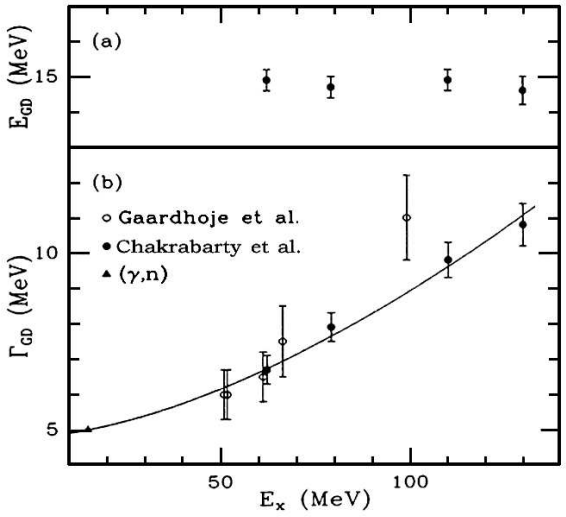

Fig. 2. The systematics for the energy (a) and width (b) of the GDR as a function of E^*. Open symbols are from refs. [23, 24] while full circles are from ref. [25]. The full line corresponds to the parametrization of the width given by eq. (6).

$E^* = 60$ MeV and angular momenta up to $I \simeq 40\hbar$. Reproducing the data through a statistical calculation performed with the code CASCADE using a single Lorentzian function centered at $E_{GDR} = 15.5$ MeV called for a width $\Gamma = 6$–6.5 MeV for the three excitation energies investigated, values which were clearly in excess of the typical widths measured on the ground state.

Similar results were obtained in the study of the GDR decay from ^{111}Sn nuclei populated at $E^* = 66$ and 100 MeV excitation energies using the reaction $^{20}\mathrm{Ne} + {}^{91}\mathrm{Zr}$ at $E_{beam} = 100$ and 140 MeV [24]. The measured γ spectra and the corresponding statistical calculation are shown in fig. 1. In this case a strength corresponding to 100% of the EWSR and widths of 7.5 and 11 MeV, respectively, were needed to reproduce the γ-ray spectra. Therefore, the results of these experiments, shown as open symbols in fig. 2, pointed to a progressive increase of the width with excitation energy at least up to $E^* = 100$ MeV. The authors suggested two possible interpretations for such an increase as due either to an increase of the GDR damping width with E^* and/or spin I or to a change in deformation.

The systematic study of the GDR properties in Sn isotopes was extended by the work of Chakrabarty *et al.* [25] at higher excitation energies ($E^* = 130$ MeV) and spin. The results concerning the centroid energies and widths are shown in fig. 2 as full circles. Within the experimental errors, the centroid energy of the GDR as extracted from best fits to experimental data are independent of excitation energy while the absolute value seems to be slightly lower than the one measured on the ground state. The width of the resonance was observed to increase with excitation energy although less strongly than reported in the previous work, the discrepancy being relevant only for $E^* = 100$ MeV. Different calculations were performed to

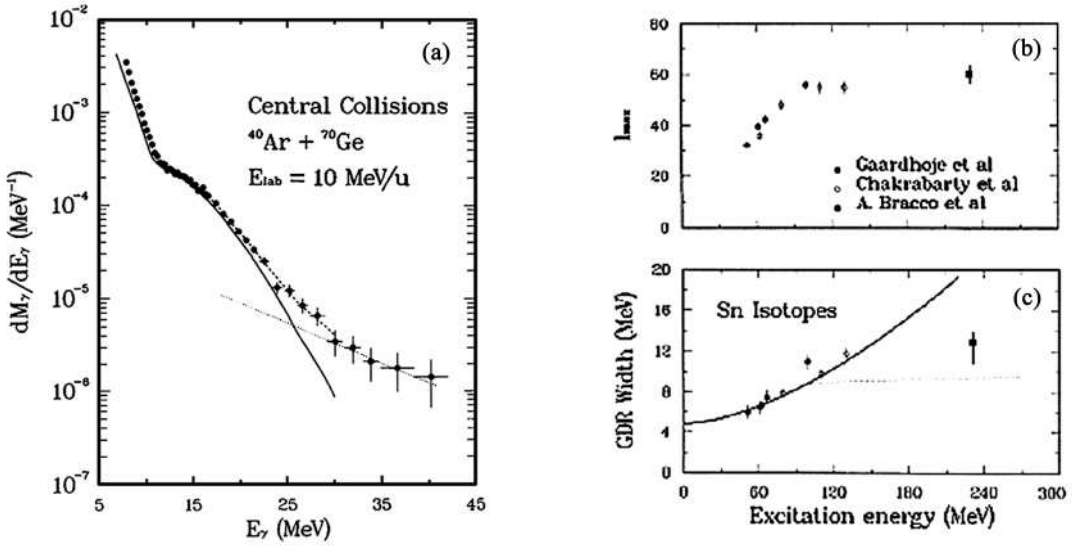

Fig. 3. a) Gamma spectrum measured in coincidence with fusion events from the reaction $^{40}\mathrm{Ar} + {}^{70}\mathrm{Ge}$ at $E_{lab} = 10A\,\mathrm{MeV}$. The full line represents the statistical calculation, the dotted line indicates the bremsstrahlung contribution while the dashed line is the sum of the previous two. b) The trend of the maximum angular momentum populated in the different fusion reactions leading to Sn isotopes as a function of excitation energy. c) The systematics of the GDR width measured on $^{108-112}$Sn isotopes as a function of excitation energy. The width value at $E^* = 230\,\mathrm{MeV}$ is the one measured by Bracco *et al.* [26] suggesting the width saturation. The full line corresponds to the parametrization of the width given by eq. (6).

investigate the sensitivity of the results to the level density parameter adopted. Small differences were observed and included in the estimated error bars. The average width trend, including the ground-state value, can be well accounted for by the relation

$$\Gamma = 4.8 + 0.0026E^{1.6}\,\mathrm{MeV}, \tag{6}$$

where the first constant represents the ground-state value. Such a trend is in qualitative agreement with calculations performed on ^{108}Sn at high spin and temperatures which predict a width increase reflecting the increase of deformation at higher angular momenta and the progressive importance of thermal fluctuations of the nuclear shape [16]. In particular, Sn isotopes are predicted to evolve from spherical towards oblate shapes with increasing spin and temperature. Thermal fluctuations wash out the structures of the absorption strength function calculated for fixed deformation inducing a broadening and a smoothing of the strength function.

It is important to mention at this point that, while a clear trend as a function of excitation energy is observed for the width, each single statistical model calculation used as a comparison to estimate the GDR parameters was performed with a fixed width all along the decay chain. Therefore, the extracted parametrization reproduces the trend for the width averaged over the decay cascade. A proper treatment of the problem calls for the inclusion of the energy and spin dependencies of the width in the calculation. Chakrabarty and co-workers investigated these dependencies and found that a good fit to the data can be obtained assuming [25]

$$\Gamma = 4.5 + 0.0004E^2 + 0.003I^2. \tag{7}$$

An abrupt change to the smooth increase of the GDR width with excitation energy observed up to 130 MeV was found in the study of the GDR structure at about $E^* = 230\,\mathrm{MeV}$. In this experiment performed using an ^{40}Ar beam at $10A\,\mathrm{MeV}$ the GDR gamma decay was investigated in ^{110}Sn nuclei and a width similar to the one previously measured at 130 MeV was observed indicating the onset of a saturation effect above 130 MeV [26].

At $10A\,\mathrm{MeV}$ beam energy the reaction dynamics are still dominated by the mean field which leads, for central collisions, mainly to complete-fusion events. However, modifications of the mean-field dynamics due to the effect of nucleon-nucleon collisions occur leading also to incomplete-fusion events characterized by a partial transfer of nucleons from the lightest to the heaviest partner of the collision which affects the final excitation energy and mass of the hot system produced. It is no longer straightforward to ascertain the excitation energy and spin distribution populated in the reaction. The higher bombarding energy also induces a new high-energy component in the γ-spectrum due to nucleon-nucleon bremsstrahlung in the first stages of the reaction. This component must be understood and subtracted before drawing conclusions on the GDR characteristics. A proper identification of the reaction mechanism and of the initial masses and excitation energies are needed in order to characterize the emitting source and follow the evolution of the GDR properties. Bracco and co-workers [26] used, in the experiment, two Parallel Plate Avalanche Counters (PPAC) to detect the reaction products in coincidence with γ-rays. Such a setup yields a measurement of the linear momentum transfer (LMT) from the projectile to the compound system. Complete-fusion events are characterized by 100% LMT.

Only such events were retained in the analysis and the gamma spectra were built accordingly. Figure 3 displays the γ-ray spectrum measured in ref. [26] which shows a clear bump associated to the GDR decay and, at higher energies, the contribution arising from bremstrahlung γ-rays originating from nucleon-nucleon collisions in the first stage of the reaction. The full line represents the statistical model calculation performed assuming a Lorentzian shape for the GDR with 100% of the EWSR, a centroid energy of 16 MeV and a width of 13 MeV constant over the whole decay path. The dotted line is the estimate of bremsstrahlung contribution while the dashed one indicates the sum of the both statistical and bremsstrahlung contributions which nicely reproduces the whole spectrum. On the right side of fig. 3 the GDR width systematics for Sn isotopes is shown including the new result at $E^* = 230$ MeV. Its value is similar to the one extracted at $E^* = 130$ MeV suggesting a saturation of the effects which lead to the observed increase at lower excitation energy. Thermal fluctuations of the nuclear shape are expected to increase with the temperature of the emitting system and therefore the observation of a saturation suggests a different origin as the main contribution to the width increase. As already observed, angular momentum drives the nucleus towards shape modifications leading to prolate or oblate configurations which become stable at high spin. In fusion reactions the transferred angular momentum increases with beam energy reaching the maximum angular momentum a nucleus of mass $A \sim 110$ can sustain before fissioning at about $E^* \sim 100$ MeV. In fig. 3 the trend of maximum angular momenta populated in the reactions investigated is compared to the width increase in the same excitation energy region. The similarities observed in the two curves drove the authors to suggest that the angular momentum is the main effect for a width increase.

Evidence for a saturation of the width was also obtained by Enders *et al.* studying the GDR gamma decay in nuclei populated in deep inelastic reactions [27]. They studied the system ^{136}Xe + ^{48}Ti at 18.5A MeV and measured the gamma-rays in coincidence with binary events. In order to investigate the excitation energy dependence of the GDR width, three different regions of excitation energy were selected and the gamma-ray spectra built accordingly. The results concerning the width show that a value of about 10 MeV reproduces the spectra at all excitation energies. Such a value is lower than the one measured by Bracco *et al.* [26] and the results seem to be insensitive to the particular choice of level density adopted in the statistical calculation. Further evidence for the width saturation came from the work of Hofmann *et al.* [28] who investigated the GDR properties using the 12.5 and 17.5A MeV ^{16}O beam impinging on the ^{118}Sn target. Assuming complete-fusion reactions, nuclei at excitation energies of 160 and 230 MeV, respectively, were populated [28]. The comparison of experimental spectra with statistical calculations indicated that a width value of 10.5–11 MeV led to a good reproduction of the data. Such values are in agreement, within the errors, with Enders' results. However, the systematics of momentum transfer

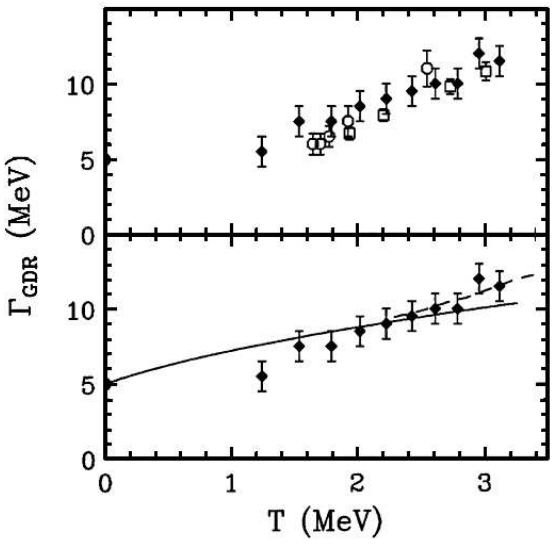

Fig. 4. Comparison of the GDR width extracted from 50A MeV α-particle inelastic-scattering experiment (full symbols) on ^{120}Sn [29] and from fusion reaction data (open symbols) on $^{108-112}$Sn nuclei [23–25]. The lower part shows the comparison of the α inelastic-scattering experiment results with adiabatic coupling calculations [32] shown as a full line. The dashed line includes the contribution to the width due to particle evaporation width [35].

indicates, for reactions at 12.5 and 17.5A MeV beam energy, an average value of 90% LMT. Calculations including corrections for incomplete momentum transfer led to differences of about 5% for the width, a value which did not affect the conclusions concerning the saturation [28]. However, this systematics of average momentum transfer was built measuring recoil velocities whose distribution becomes broader with increasing beam energy and they might not take properly into account pre-equilibrium emission which could affect the excitation energy and mass of the equilibrated system.

Once the systematics was established using fusion reactions, the next step was to attempt to disentangle the effects of the two parameters driving the width evolution, temperature and angular momentum.

A way to populate nuclei at well-determined temperatures and low angular momentum was proposed by Ramakrishnan *et al.* [29]. They used the inelastic scattering of α-particles at 40 and 50A MeV as a tool to populate ^{120}Sn nuclei in the excitation energies range of 30–130 MeV and low angular momentum states (about 15$\hbar$ on the average) which allowed one for the first time to study the effects of large amplitude thermal fluctuations and angular momentum separately. The initial excitation energy of the target nuclei was determined from the energy loss of the scattered α-particle and the GDR evolution was followed gating on different windows of energy loss. Data analysis indicated a monotonic increase of GDR width with target excitation energy for both beam energies. Besides, the results were found in good agreement

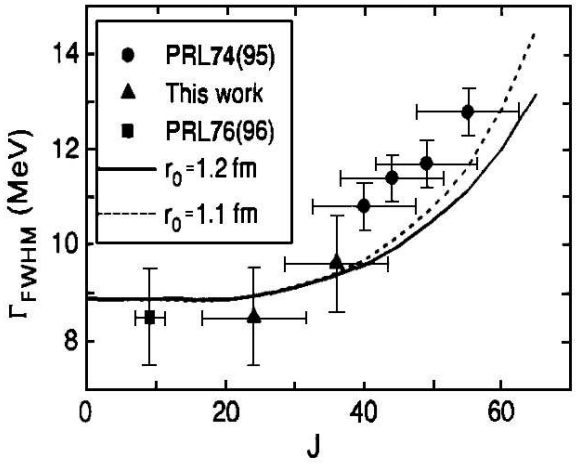

Fig. 5. Evolution of the width as a function of angular momentum at $T \sim 2\,\mathrm{MeV}$ [30]. The solid line represents a calculation of the width evolution with spin assuming a moment of inertia of the nucleus equal to the rigid-rotor value while the dashed line is a similar calculation assuming a reduction of 16% in the rigid-rotor value [30].

with the existing systematics built on fusion data as shown in fig. 4. The agreement found up to $E^* = 130\,\mathrm{MeV}$ in the data sets extracted using different reaction mechanisms which populate nuclei in rather different spin regions suggests that the increase in the width is mainly driven by temperature effects differently from what was previously suggested by Bracco *et al.* [26].

In order to evaluate the angular-momentum dependence of the GDR width at a fixed temperature fusion evaporation experiments were used to populate hot Sn nuclei at about $T \simeq 2\,\mathrm{MeV}$ [30]. Differently from previously described fusion-evaporation experiments a multiplicity filter was used to select fusion events according to different average spin regions. The results, together with other exclusive measurements showed that the width measured at $T \simeq 2\,\mathrm{MeV}$ is roughly constant up to spin $J \leq 35\hbar$ and then progressively increases up to the highest measured spin as shown in fig. 5 [30,31]. This trend is rather well reproduced by the calculations based on adiabatic theory of thermal shape fluctuations [19,32].

The results clearly suggest that the observed disagreement in the conclusions concerning the dominance of angular momentum and temperature effects on the width increase could be attributed to the different region of angular momentum investigated by the two types of experiments. In fact, the results of ref. [30] indicate that the influence of angular momentum on the width becomes really important only above $I \sim 35\hbar$, as is the case for the highest excitation-energy fusion data [26]. Such a conclusion finds a theoretical support in the results of adiabatic theory of thermal shape fluctuations which predicts the same effect.

Thermal shape fluctuation calculations give also a reasonable description of the overall GDR width increase as a function of the system temperature as shown in fig. 4. The temperatures indicated are the initial temperatures of the compound nuclei. Taking into account a weighted average of the temperatures of nuclei contributing to the GDR gamma emission over the various decay steps would reduce these values by at most 0.6 MeV [33,34]. The inclusion of the evaporation width contribution [35] to the GDR width due to the finite width of both initial and final nuclear states involved in the GDR decay improves and extends the agreement between data and theory up to the highest E^* points (see fig. 4). However, the calculations are not able to reproduce the data trend below $T < 1.2\,\mathrm{MeV}$. The recent observation of a width close to the ground-state width at very low temperatures made the scenario a bit more confused casting some doubts on the validity of the calculations in the low-temperature region. Data from the ^{17}O inelastic scattering on ^{120}Sn [20] extracted at $T = 1\,\mathrm{MeV}$ indicate that the GDR width in ^{120}Sn is 4 MeV, a value similar to the one extracted on the ground state compounding the difference with the calculation made in the framework of the standard theory of shape fluctuations [20]. This result cannot be currently explained in the framework of the thermal shape fluctuations [20,21]. Some new results were recently published also about the angular-momentum dependence of the width. In particular, an experiment on ^{86}Mo using fusion reactions did not show any dependence of the width on angular momentum which was measured to be constant up to $30\hbar$ at $T \simeq 1.3\,\mathrm{MeV}$ [36]. The experimental evidence and theoretical framework discussed up to this point suggest that both angular momentum and temperature are effective in driving the nucleus towards more deformed or elongated shapes which influence the GDR width which becomes progressively broader with increasing excitation energy. At about $E^* \simeq 130\,\mathrm{MeV}$ the system reaches the limiting angular momentum for a nucleus of mass $A \approx 120$ and this strongly affects the increase of the GDR width which seems to saturate. A smooth increase is instead predicted by thermal models due to the increase of the temperature effects which should lead to a $T^{1/2}$-dependence.

More recently some doubts were cast on the excitation energy determination in the fusion reactions. In particular it was pointed out that a proper determination of pre-equilibrium emission is mandatory in the estimate of the E^* of the system whose uncertainties could affect the conclusions concerning the width saturation. Recently, protons and α-particle pre-equilibrium emission has been established down to $E_{beam} = 7A\,\mathrm{MeV}$ [37,38]. The measurements show that, on the average, the compound nucleus excitation energy is reduced by few percent at 7–8A MeV and about $\simeq 20\%$ at 11A MeV using asymmetric reactions populating the $A \sim 115$–118 mass region [37,38]. At the same time, the mass of the compound system is reduced by a few units relative to complete fusion. The inclusion of the pre-equilibrium emission in the energy balance lowers the computed temperatures and increases the extracted GDR width and strength because of the lower excitation energy value used in statistical model calculations to reproduce the gamma-ray spectra. The ev-

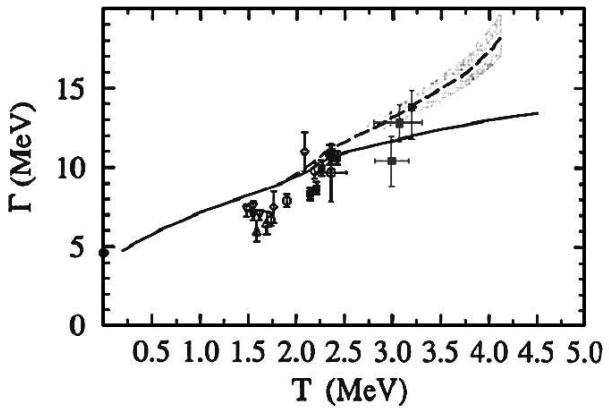

Fig. 6. Evolution of the width as a function of excitation energy applying the correction for pre-equilibrium emission to the highest E^* points [39] which were extracted in refs. [26,27].

idence of a pre-equilibrium emission already at $8A$ MeV suggested a re-analysis of the data taken above $10A$ MeV due to an overestimation of the initial excitation energy which, in some cases, was estimated assuming complete fusion. When excitation energies and temperature are recomputed including the pre-equilibrium emission the results of refs. [26,27] indicate that the width is still increasing up to temperatures $T \sim 3.2$ MeV as shown in fig. 6 [38, 39]. The calculations based on adiabatic thermal shape fluctuations including the contribution to the GDR width coming from the evaporative decay support this conclusion (see fig. 6) up to $T \simeq 3$ MeV [19]. However, recent experimental findings showed a significant difference in pre-equilibrium emission between symmetric and asymmetric reactions which affects the final excitation energy of the system and, therefore, the conclusions concerning the GDR width saturation [40].

From the analysis of all the experimental findings up to an excitation energy of 200 MeV a scenario emerges where the strength of the GDR retains 100% of the EWSR and the width progressively increases due both to temperature and spin effects, the latter mainly playing a role above 35–40$\hbar$. The observed saturation of the width above about $E^* = 150$ MeV is due to limiting angular momentum from the opening of the fission channel. There is no strong evidence of a saturation of the width with increasing temperature at fixed angular momentum.

Dynamical effects start to set in at the highest end of the energy range discussed. They have non-negligible effects on the conclusions and are not completely under control. This problem will be exacerbated when moving to even higher energies in the next section.

6 Disappearance of the GDR above $E^* \sim 200$ MeV

The study of the GDR properties at high excitation energies was mainly focused in the Sn mass region where broad systematics was collected in different experiments. The experimental investigation was undertaken by the different groups in a rather coherent way since in all experiments gamma-rays were detected in coincidence with reaction products. Typically, PPACs were used to identify incomplete-fusion events where only part of the light projectile is transferred to the target, through the simultaneous measurement of energy loss and time of flight of the residues. Broad distributions of recoil velocities were detected reflecting a range of momentum transfers leading to systems with different masses and excitation energies whose values can be estimated using a massive transfer model [41]. This is a very attractive feature of intermediate-energy heavy-ion collisions since, as long as the hot nuclei can be properly characterized, the broad excitation energy distribution measured can be used to follow the evolution of the gamma emission as a function of excitation energy in a single experiment. The recoil velocity distributions were sorted in bins corresponding to different average excitation energies and gamma spectra were built accordingly. The analysis of the gamma spectra was usually carried out using a statistical decay code which treats the statistical emission of γ-rays, neutrons, protons, alpha particles and in a few cases also a fourth particle (like a deuteron) from an equilibrated compound nucleus. The bremsstrahlung γ-ray contribution which dominates the high-energy part of the spectrum was estimated fitting the spectral shape with an exponential function above about 30 MeV. Since it gives also a sizeable contribution to the region below 30 MeV which is difficult to determine experimentally and which affects the estimate of the GDR yield, the exponential fit is extrapolated down to low energies. Eventually, this contribution was subtracted from the experimental spectrum in order to obtain the GDR gamma yield and to allow for a direct comparison with statistical calculations folded with detector response. However, even though the basic approach is the same, the authors followed, in the data analysis, different hypothesis concerning the GDR properties at high E^*, which lead, at least for some time, to controversial conclusions. In the following we will show the results of the different experiments, the procedure adopted in the analysis and eventually the comparison with theoretical models which provides the present understanding of the GDR behavior at very high temperature.

The first pioneering work to investigate the persistence of collective motion at very high excitation energies was performed by Gaardhøje *et al.* who studied the reaction $^{40}\mathrm{Ar} + {}^{70}\mathrm{Ge}$ at 15 and $24A$ MeV beam energies [42]. Hot nuclei formed in incomplete-fusion reactions were populated at average excitation energies $E^* = 320$ MeV and $E^* = 600$ MeV for the two reactions. These estimates, based on average momentum transfer, did not take properly into account pre-equilibrium particle emission which affects significantly the excitation energy value in the case of the reaction at $24A$ MeV. However, even if corrections should be applied to extract a proper value of E^* for the emitting system, the general conclusions of this work remain the same, the excitation energy of the system

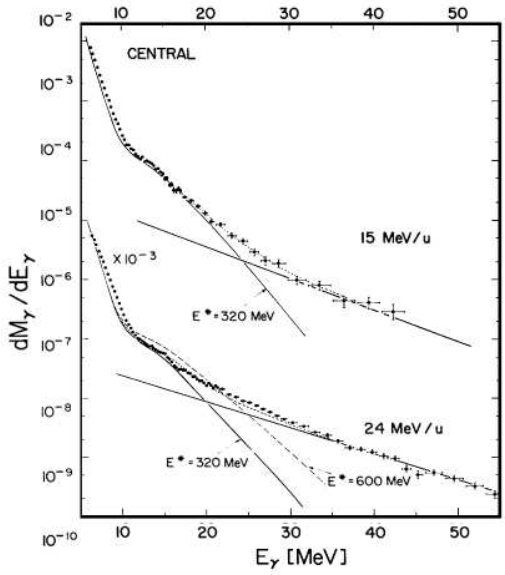

Fig. 7. Gamma spectra measured in the reactions ^{40}Ar + ^{70}Ge at 15 and 24A MeV. The full line represents the statistical model calculation performed at $E^* = 320$ MeV while the dashed line is a calculation assuming $E^* = 600$ MeV. Dotted lines are the sum of statistical plus bremsstrahlung contributions [42].

populated at 24A MeV is in any case much higher than 300 MeV.

The γ-ray spectra were reproduced assuming for the GDR a single Lorentzian shape with a centroid energy $E_{GDR} = 15.5$ MeV, a width $\Gamma = 15$ MeV and 100% of the EWSR. As it can be seen in fig. 7, the statistical calculation reproduces the gamma-ray spectrum measured at 15A MeV while a strong over-prediction of the GDR gamma yield is observed in the case of 24A MeV. These data indicated, for the first time, the existence of a suppression of the γ emission at high excitation energies [42] compared to the prediction of the statistical model which was interpreted as a loss of collectivity of the system. The spectrum measured at 24A MeV was found similar to the one measured at 15A MeV and could be reproduced assuming an excitation energy $E^* = 320$ MeV, a value much lower than the estimated one. Such an approach lead to the interpretation of the sudden disappearance of the GDR with increasing excitation energy. These observations suggested, for the first time, the existence of a limiting temperature $T \sim 4.5$ MeV for the collective motion.

Further evidence for the suppression of the γ yield at very high excitation energies was then found studying the reactions ^{40}Ar + ^{92}Mo at 21 and 26A MeV [43], ^{36}Ar + ^{90}Zr at 27A MeV [44] and ^{36}Ar + ^{98}Mo at 37A MeV [45]. These results could not be explained in the framework of statistical models because at higher excitation energies the number of emitted gamma-rays should increase due to the higher number of steps available for the GDR to compete with particle emission. Interest for this new problem spread through the theoretical community. Different approaches were proposed to explain the quenching of the GDR. The different ideas point to two main effects which could lead to a saturation of the GDR gamma yield at high excitation energy, either a suppression of the GDR or a rapid increase of the width. In the following section we will first describe the different theoretical models and then we will come back to a more detailed description of the experimental results.

6.1 Theoretical models: yield suppression

The statistical model used to reproduce the gamma-ray spectra emitted in the decay from a hot compound nucleus is based on the assumption that the nucleus survives long enough to reach thermal equilibrium before decaying. This hypothesis, valid for nuclei at low excitation energies, may not always be fulfilled at very high excitation energies where the time needed for the system to equilibrate the different degrees of freedom, in particular the collective ones, could become longer than the nucleus lifetime [46]. In this case the system will start to cool down by particle emission before being able to develop a collective oscillation.

The observation of a GDR quenching at high excitation energies has been interpreted by some theoreticians as a possible evidence of such pre-equilibrium effects. The time scale governing the GDR equilibration can be related to the GDR spreading width $\Gamma^{\downarrow}$. Since the particle evaporation width Γ_{ev} increases as a function of the temperature according to the statistical model predictions, as shown in fig. 8, the existence of the GDR above a certain excitation energy depends on the relative size of the spreading and evaporative widths [47]. The model suggested by Bortignon *et al.* [47] is based on the assumption

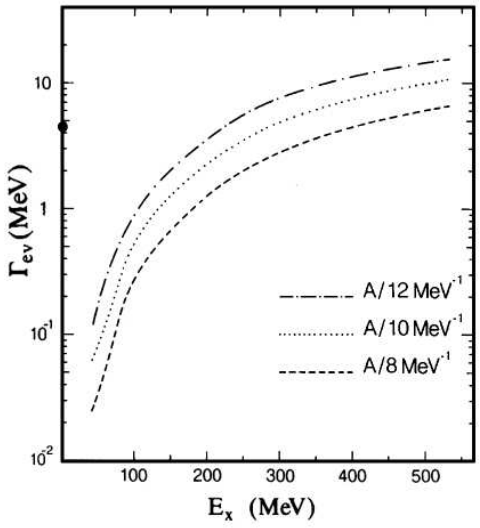

Fig. 8. Particle evaporation widths as a function of excitation energy estimated in the framework of the statistical model for three values of the level density parameter ranging from $a = A/8$ to $a = A/12$ [47]. The full symbol represents the value of the $\Gamma^{\downarrow}$ of the GDR measured on the ground state in ^{108}Sn.

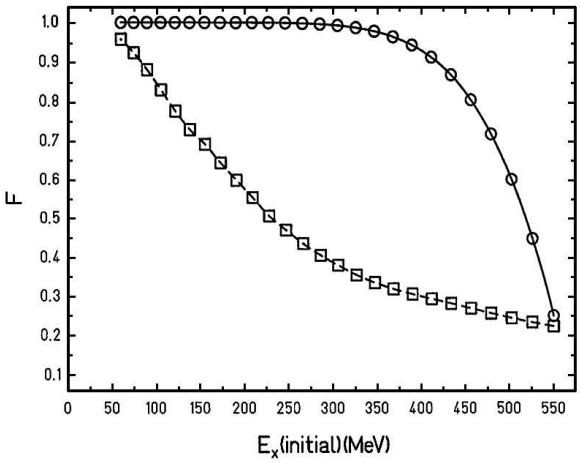

Fig. 9. Comparison of GDR suppression factors as a function of excitation energy for a system with $E^* = 550\,\mathrm{MeV}$. Circles indicate the results obtained estimating the suppression factor according to eq. (10) while squares are obtained using the relation given by eq. (8) [39].

that the compound nucleus states can exist in two different classes, with or without the GDR. Assuming that GDR states are not populated at the beginning of the reaction, the excitation energy at which the spreading width and evaporative width are comparable $\Gamma_{ev} \sim \Gamma^{\downarrow}$ defines a critical temperature for the existence of collective motion [47]. Above this temperature, in fact, the compound nucleus will evaporate particles before the GDR can be present in thermal equilibrium reducing its temperature. This affects the GDR yield which will be reduced by an amount related to the time needed to develop the collective oscillation relatively to the particle decay time. The model predicts a hindrance factor for the GDR emission dependent on excitation energy given by

$$F = \frac{\Gamma^{\downarrow}}{\Gamma^{\downarrow} + \Gamma_{ev}}\,, \tag{8}$$

where Γ_{ev} increases rapidly with temperature. The fulfilment of the condition $\Gamma_{ev} \geq \Gamma^{\downarrow}$ relies on the temperature dependence of the spreading width as compared to the particle decay width. Since a suppression of the GDR was observed above $E^* \simeq 250\,\mathrm{MeV}$ this was interpreted by Bortignon and co-workers as an indication that, at this excitation energy which corresponds to a temperature $T \sim 5\,\mathrm{MeV}$, the condition $\Gamma_{ev} \geq \Gamma^{\downarrow}$ is fulfilled. Comparing the value $\Gamma^{\downarrow}$ measured on the ground state which is about 4.5 MeV to Γ_{ev} calculated at $E^* = 250\,\mathrm{MeV}$ which is $\sim 5\,\mathrm{MeV}$ the authors concluded that $\Gamma^{\downarrow}$ is essentially independent of temperature. Similar conclusions concerning the independence of the spreading width of the temperature can be found in the theoretical work of Donati *et al.* [48].

It has been noted that the pre-equilibrium effects might be overestimated in the preceding model due to the hypothesis of a complete absence of population of GDR states at the beginning of the reaction on which the model is based. In fact, the existence of some initial dipole oscillations in the fused system due to the long equilibration time of the charge degree of freedom has been theoretically investigated together with the excitation energy dependence of the spreading width. The calculations suggest that a suppression or an enhancement of the gamma emission could be observed depending on the initial conditions of the system out of equilibrium [49].

More recently the effect of the equilibration time for different degrees of freedom has been re-investigated [39]. Assuming that the equilibration of the collective vibration occurs with a probability given by

$$P(t) = 1 - \exp(-\mu_0 t), \tag{9}$$

where $\mu_0 = \Gamma_0/\hbar$ is a characteristic mixing rate related to the spreading width and t is the time elapsed in the decay process, one can estimate the inhibition factor for the GDR decay et each step of the decay. At the first step the time to consider in eq. (9) will be the mean lifetime of the compound nucleus $t_{ev} = \hbar/\Gamma_{ev}$. For the n-th decay step the probability will be modified by the elapsed time which can be estimated as $t \sim \sum_{i=1}^{n} t_{ev}(i)$, where $t_{ev}(i)$ is the mean lifetime for the i-th decay step. Then the suppression factor is reduced and becomes [39]

$$F_n \sim 1 - \exp\left(-\Gamma_0 \sum_{i=1}^{n} \Gamma_{ev}(i)^{-1}\right). \tag{10}$$

The comparison of this suppression factor with the one predicted by eq. (8) for a compound system with $E^* = 550\,\mathrm{MeV}$, mass $A = 110$, $\Gamma_0 = 4\,\mathrm{MeV}$ and assuming $A/a = 11$ is shown in fig. 9. The different points in the figure are computed assuming an energy release per decay step given by $\Delta E = B_n + 2T$, where $B_n \approx 9\,\mathrm{MeV}$ and $T = \sqrt{(E/a)}$ [39]. As it can be observed, the two suppression factors are similar at the first step but then, during the de-excitation process, eq. (10) predicts a rapid decrease of the suppression which becomes negligible already around $E^* = 300$–$350\,\mathrm{MeV}$ while eq. (8) gives still a not negligible suppression at $E^* \sim 100\,\mathrm{MeV}$.

A different origin of the suppression of the GDR γ emission was suggested by Chomaz [50]. In his model the explanation of the quenching effect is again related to the different time scales which come into play in the emission process. Differently from the previous approach, he suggests to take also into account the period of one oscillation of the emitting system given by $T_{GDR} = 2\pi/E_{GDR}$. In fact, in order to be able to emit characteristic photons the system needs to make at least one full oscillation without perturbation of its dipole moment. Conversely, the associated spectrum cannot show a characteristic frequency. Since particle emission can induce fluctuations of the dipole moment the times which come into play and compete are the time between the sequential emission of two particles t_{ev} and the period of one collective oscillation T_{GDR}. The condition $t_{ev} \simeq T_{GDR}$ defines the threshold towards a chaotic regime where the collective oscillation is suppressed. The probability to make at least one oscillation can be computed and a GDR quenching factor can

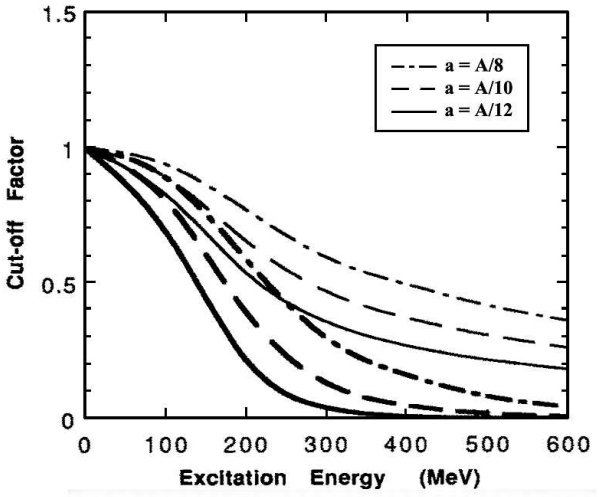

Fig. 10. Evolution of quenching factors predicted for Sn nuclei as a function of excitation energy for different values of the level density parameter. Thick lines show the reduction factor predicted in ref. [50] while thin lines are predictions made according to ref. [47].

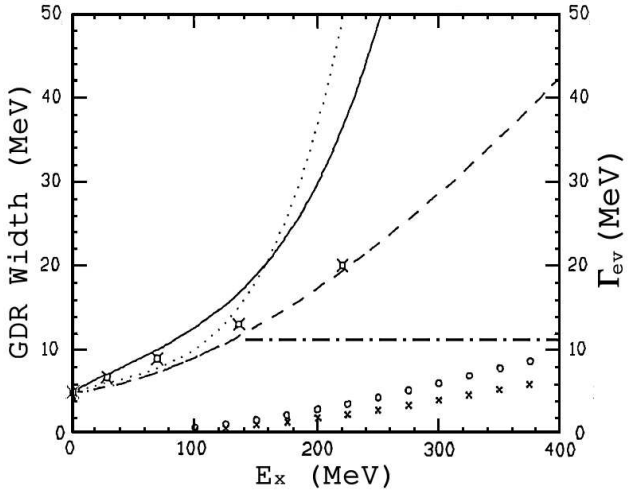

Fig. 11. Excitation energy dependence of the GDR width for Sn isotopes. Open square symbols represent the results of the calculations of Bonasera *et al.* [53]. The dashed line is the extrapolation to higher energies of the width parametrization given by eq. (6). The solid line is the estimate for the width increase according to Smerzi *et al.* [51], the dotted one is a fit of the width trend extracted from ref. [43] and the dot-dashed one is a parametrization assuming a constant width of 11 MeV above $E^* = 130$ MeV. In the same figure the Γ_{ev} values calculated for level density parameters $a = A/12$ (circles) and $a = A/10$ (crosses) are shown.

be extracted. It depends on the resonance energy and the evaporative width according to the relation

$$F = \exp\left(\frac{-2\pi\Gamma_{ev}}{E_{GDR}}\right). \qquad (11)$$

The excitation energy dependence of the GDR suppression factor is shown in fig. 10 for Sn nuclei. In the same figure the suppression factor proposed in ref. [47] is shown as a comparison. The effect of different values of the level density parameter on the suppression factor is also shown. Chomaz's approach to explain the GDR quenching leads to a suppression factor whose effects are much stronger than those predicted in ref. [47]. In particular, a sizeable quenching is predicted already between 150–200 MeV excitation energy, an excitation energy region where the GDR was measured to retain 100% of the EWSR.

6.2 Theoretical models: width increase

A completely different interpretation of the quenching effect was developed following the idea of a GDR width strongly increasing with the temperature. This argument is not in disagreement with the apparent saturation of the width at about 12–13 MeV observed above 250 MeV excitation energy in different experiments and, as we will see, its implication should give a clear signature in the gamma-ray spectrum which is not predicted by models which interpret the GDR quenching in terms of yield suppression. Such difference will become the key issue to segregate between the two theoretical interpretations of the GDR quenching.

In the attempt to reproduce the experimental data two different explanations leading to a rapid width increase at high excitation energy were put forward. Following a semiclassical approach solving the Vlasov equation with a collision relaxation time, Smerzi *et al.* [51] studied the interplay between one- and two-body dissipation on the damping of collective motion. They evaluated the escape width $\Gamma^{\uparrow}$ and the spreading width $\Gamma^{\downarrow}$ contributions as a function of temperature. The escape width was found to be of the order of few hundred keV while a strong increase of the spreading width was observed as a function of the temperature [51]. Such an effect is due to two-body collisions which become increasingly important with temperature because of the suppression of Pauli blocking.

The excitation energy dependence of the GDR width for Sn isotopes is shown in fig. 11 as open squares and can be described reasonably well by the dashed line which is an extrapolation to higher energies of the Chakrabarty parametrization for the width found at lower excitation energies [52,53]. At about $E^* \simeq 230$ MeV the calculations predict a GDR spreading width of the order of the resonance energy and the contribution to the gamma-ray spectrum around the GDR energy becomes small. In fact, the γ-rays are spread out over a very large decay energy range. Therefore, the conclusion is that the GDR progressively disappears with excitation energy due to this broadening of the resonance. This interpretation should be able to explain the quenching of the γ yield and paradoxically is not in contradiction with the *apparent* width saturation. The analysis of the spectral shape in a region above the resonance should reveal the contributions not present at lower excitation energies. This part of the spectrum then

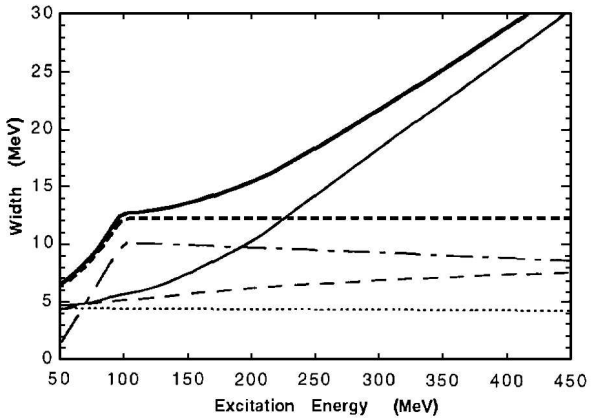

Fig. 12. Evolution of the total GDR width and its various components in Sn isotopes as a function of excitation energy. The thick solid line displays the total width predictions according to the parametrization suggested in ref. [54] including the particle evaporation width contribution [35]. The thick dashed line represents the standard prediction assuming the saturation at 12 MeV. The thin lines show the contribution to the width due to the various components. In particular, the thin solid line represents the intrinsic width including the particle evaporation width contribution while the dotted one shows the intrinsic width.

becomes of great importance to draw conclusions concerning the validity of the different models.

A different idea based on the width increase was proposed by Chomaz to explain the observed saturation of the yield [35,50]. The key issue is that each nuclear level involved in the GDR gamma decay has a finite lifetime τ due to particle evaporation. The value of the lifetime induces, according to the Heisenberg uncertainty principle, a width of each nuclear level of the order of $\hbar/\tau$. Therefore the transition energies between nuclear levels, like gamma-ray energies, cannot be determined to better than $2\hbar/\tau$. This indetermination affects the total width of the resonance but not the position of the centroid. Assuming for each nuclear level a width equal to the evaporation width of the compound system Γ_{ev} the total width of the GDR should contain the contributions coming from the spreading width and the natural width of the elementary gamma transition according to the relation [35]

$$\Gamma_{GDR} = \Gamma^{\downarrow} + 2\Gamma_{ev}\,. \tag{12}$$

While at low excitation energies the contribution arising from Γ_{ev} is negligible the statistical model predicts a strong increase of the particle evaporation width with excitation energy. In fig. 12 the evolution of the total GDR width calculated including the evaporation width effect is shown as a full thick line. In the same figure the contribution arising from the $2\Gamma_{ev}$ term is shown as full thin line. The comparison with the prediction assuming a saturating width according to the experimental observation shows that the new contribution starts to be significant in the region of $E^* \simeq 150$–200 MeV, becoming the dominant one above $E^* \sim 300$ MeV.

The strong increase predicted by both models could, in principle, explain the disappearance of the GDR at high excitation energies but the comparison of the experimental data with the results of statistical calculations including model prescriptions will show significant discrepancies which cannot be accounted for assuming a width increasing with temperature.

6.3 Evidence for the yield saturation

Now we come back to the experimental evidences for the yield saturation discussing in detail the results of different experiments performed in the Sn region together with the different approaches adopted to interpret the data. Historically, after the first evidence for the yield saturation observed by Gaardhøje, this issue was re-investigated at RIKEN by studying the gamma-ray spectra measured in coincidence with evaporation residues produced in the reactions $^{40}\mathrm{Ar} + {}^{92}\mathrm{Mo}$ at 21 and $26A$ MeV [43]. At these bombarding energies incomplete fusion is the dominant reaction mechanism for central collisions and, therefore, the characterization of the emitting source becomes rather complex. Two methods were used to determine the excitation energy of the system: one based on the recoil velocities and the other on the measurement of neutron spectra. Gates on recoil velocity were applied to select nuclei with different average excitation energies whose values were estimated using a massive transfer model. Neutron and gamma-ray spectra were built accordingly. Neutron spectra were analyzed assuming the emission from two moving sources, one associated to the compound nucleus and the other to pre-equilibrium [55]. The results showed that both the temperature and the multiplicity of neutrons emitted from the compound nucleus source increase smoothly as a function of residue velocity [43,55] supporting the interpretation of a statistical emission from an equilibrated system formed at progressively higher excitation energy.

Gamma-ray spectra were extracted for both reactions and all velocity bins. The GDR gamma yield, integrated in the region $12 \leq E_{GDR} \leq 20$ MeV after bremsstrahlung subtraction, was observed to be almost constant, within the error bar, in the whole region above 250 MeV excitation energy [43,56], see fig. 13. The spectra were then analyzed using the standard statistical calculation assuming for the GDR a centroid energy $E_{GDR} = 15.5$ MeV, a width $\Gamma_{GDR} = 20$ MeV and full strength of the EWSR. The comparison clearly showed that the statistical calculation strongly overshoots the data in the GDR region.

In order to reproduce the spectra the authors proposed to include the energy dependence of the GDR width in the statistical calculation [43]. They showed that, taking into account the width variation at each step of the decay process, statistical model calculations were able to reproduce the γ-ray spectra at different E^* without introducing a reduction of the EWSR strength above a critical excitation energy. This was a really new approach since, traditionally, each single calculation was performed assuming a width constant during the de-excitation process. The inclusion of the excitation energy dependence

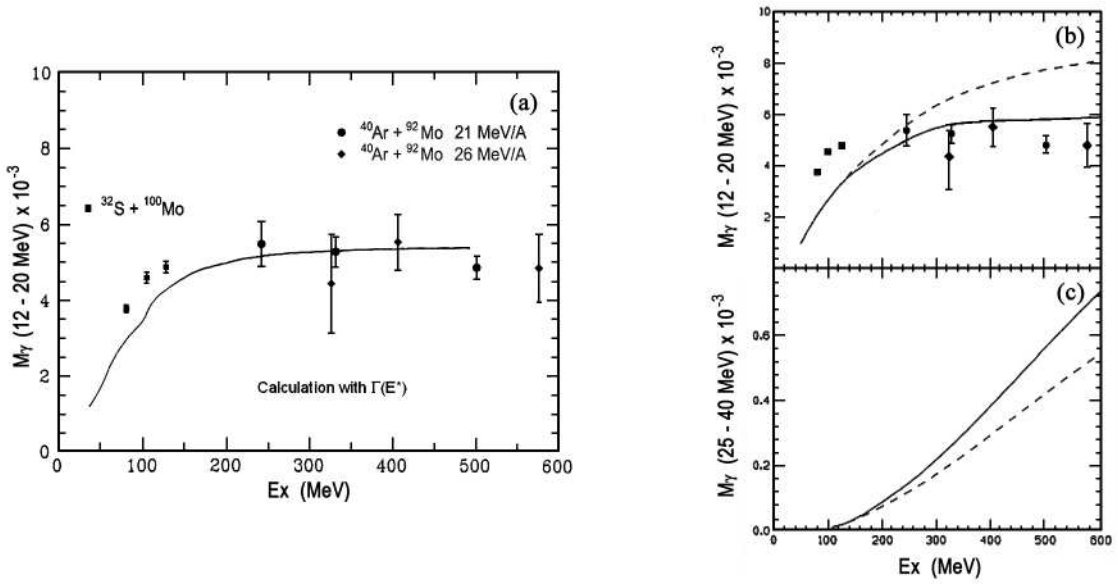

Fig. 13. a) Evolution of the gamma yield integrated in the region between 12 and 20 MeV as a function of excitation energy for different reactions. Circles correspond to 21A MeV data, diamonds to 26A MeV data while squares are from the reaction $^{32}\mathrm{S} + {}^{100}\mathrm{Mo}$ at 150, 180 and 210 MeV beam energies [56]. The solid line represents the calculation of the γ yield, integrated in the same energy region, according to the parametrization adopted in ref. [43]. b) Comparison between the same set of data and the theoretical predictions according to Smerzi *et al.* [52], (solid line) and Bortignon *et al.* [47] (dashed line) c) Same model calculation as above but in the energy region 25–40 MeV.

of the width in the calculation produces a spread of the strength function outside the GDR peak region at high E^* leading, therefore, to a quenching of the gamma yield in the GDR region. Figure 13 shows, as a solid line, a calculation of the gamma yield integrated in the region $12 \leq E_\gamma \leq 20$ MeV including the energy dependence of the width. The data trend is rather well reproduced and the differences observed at low excitation energies can be ascribed to a different initial mass of the emitting system and to a different trigger adopted [56]. While a first analysis of the spectra suggested a strong dependence of the width on E^* [43], when the effect of equilibration time was taken into account in the calculation including the factor $\Gamma_{GDR}/(\Gamma_{GDR} + \Gamma_{ev})$ [47,57] a good fit was obtained with an energy dependence very similar to the one found by Chakrabarty at lower excitation energy [56,57].

The analysis in terms of a strongly increasing width found a significant theoretical support in a series of works where a strong width increase with temperature due to 2-body collisions was predicted [51–53]. Using this model the authors were able to reproduce the overall trend of the γ yield [52,53] shown as a solid line in the right panel of fig. 13. The saturation around $E^* = 250$–300 MeV is also reproduced leading to a corresponding limiting temperature $T \simeq 4$ MeV for the GDR in the mass region $A \sim 120$.

Therefore, while there was an agreement between Kasagi *et al.* and Gaardhøje *et al.* data on the GDR quenching and on the existence of a limiting temperature $T \simeq 4$ MeV for the collective motion, the different hypotheses adopted in the analysis led to controversial conclusions concerning the reasons of the GDR quenching. The question how and why the GDR disappears was still open and the answers were found later, in the region of the spectrum above the resonance. In fact, the spread of the GDR strength function at high excitation energies predicted by a strong width increase affects the high-energy part of the spectrum where a sizeable difference in the spectral shape should be observed comparing constant width and increasing width prescriptions. In particular, a higher yield is predicted in the region $E_\gamma \geq 25$–40 MeV by calculations including a width increase as shown in the lower panel on the right of fig. 13. This region of the spectrum is rather difficult to analyze experimentally due to the presence of a significant contribution from np bremsstrahlung emission which dominates the γ-ray spectrum above 35 MeV. The bremsstrahlung contribution has to be evaluated and subtracted from the spectrum to allow for a proper determination of the GDR gamma multiplicity and to constrain different theoretical interpretations. The evaluation is typically done fitting with an exponential function the high-energy part of the spectrum ($E_\gamma \geq 30$–35 MeV) and then extrapolating the fit down to lower energies. High statistics is needed to allow for a precise determination of the slope of the bremsstrahlung component which is the crucial ingredient in the data analysis since it strongly affects the gamma yield determination. The limited statistics of the RIKEN data in the region above 25 MeV may have affected the proper determination of the bremsstrahlung contribution precluding a correct comparison of the spectral shape with statistical model calculations in this energy domain.

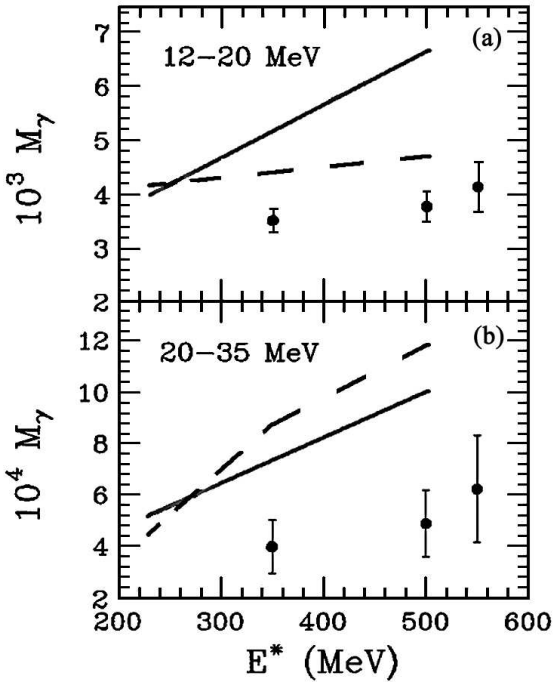

Fig. 14. a) Evolution of the gamma yield integrated in the region between 12 and 20 MeV as a function of excitation energy for the reaction ^{36}Ar + ^{90}Zr at 27A MeV [61]. Full symbols are experimental results, the full line is the prediction of the standard statistical calculation while the dashed one is the prediction of a statistical calculation including a parametrization for the width given by eq. (6) [25,61]. b) Same comparison as above but in the energy region 20–35 MeV.

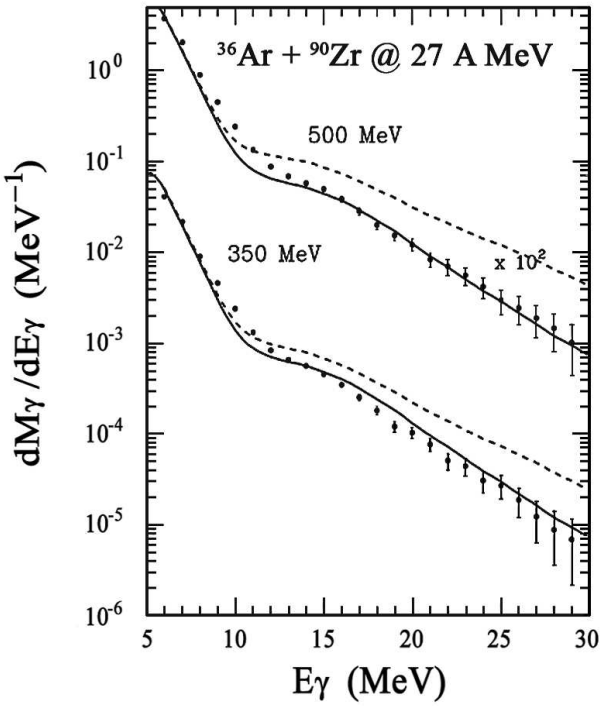

Fig. 15. Comparison of the gamma-ray spectra extracted for 350 and 500 MeV excitation energy bins after bremsstrahlung subtraction with statistical calculations [61]. The dashed lines represent the standard calculations while the full lines are the calculations including the suppression of the GDR emission above $E^* = 250$ MeV.

A clear answer to the open questions concerning the width and the strength behavior at high E^* was obtained in a set of experiments performed with the MEDEA detector [58] at GANIL and more recently at the LNS-Catania. In the GANIL experiments ^{36}Ar beams at 27 and 37A MeV impinging, respectively, on ^{90}Zr and ^{98}Mo targets were used to populate hot nuclei at excitation energies above 300 MeV [44,45]. The characterization of the hot nuclei was obtained through a complementary analysis of the recoil velocities and the study of light charged particle spectra [44,59]. The gamma spectra corresponding to the decay of systems with different average excitation energies were analyzed and the integrated gamma yield was observed to be almost constant within the error bar in the whole E^* region for each beam energy. The top panel in fig. 14 shows the gamma yield integrated in the region 12–20 MeV for 27A MeV data for the three excitation energy bins investigated. Slightly lower values were observed in the 37A MeV data.

The analysis of the spectra based on the comparison with standard statistical model calculations assuming a single Lorentzian shape for the GDR with centroid energy parametrized by $E_{GDR} = 76/A^{1/3}$, a constant width $\Gamma = 12$ MeV, a strength equal to 100% of the EWSR and a level density parameter dependent on the temperature [60] indicated a GDR quenching in both reactions. The simplest way to reproduce the data was to introduce a sharp suppression of the gamma emission above a given excitation energy, the so called cut-off energy. In the analysis of the 27A MeV data the authors reproduced the spectra extracted at all the excitation energies using the same cut-off value of 250 MeV as shown in fig. 15 [61]. A slightly lower cut-off value was needed in the case of the 37A MeV data.

In order to constrain the different theoretical interpretations and find a definitive answer concerning how and why the GDR disappears, statistical calculations including the different model prescriptions were performed and compared to the spectra. The results of the calculation, shown in fig. 16 [61], clearly indicate that models including a continuously increasing width while leading to a decrease of the yield near the centroid of the resonance clearly fail to reproduce the high-energy part of the spectra both in yield and slope. Conversely the smooth cut-off prescription based on equilibration time effects suggested in ref. [47] gives a reasonable reproduction of the data. However, recently, Snover showed that this form of the cut-off while being valid at the first step of the decay process actually overestimates the inhibition over the entire decay chain [39]. The calculation including the modified smooth cut-off (see eq. (10)) led to a larger discrepancy between data and model [39].

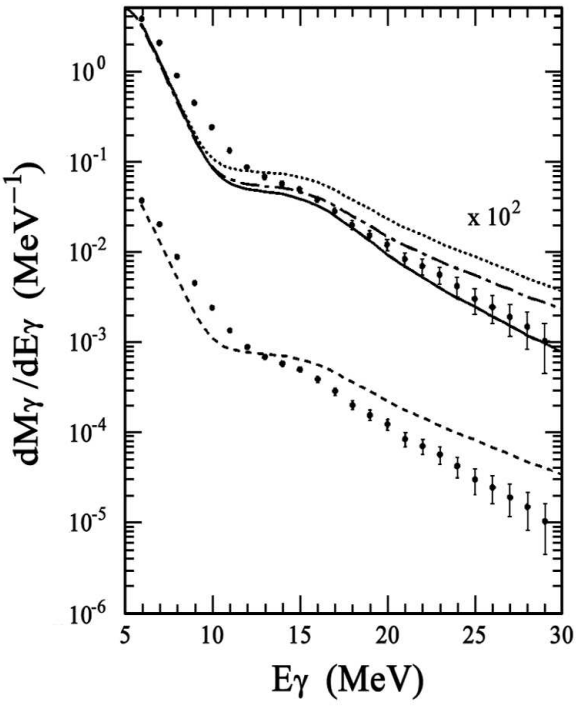

Fig. 16. Top: comparison between spectra extracted at 500 MeV excitation energy in the reaction $^{36}\mathrm{Ar} + {}^{90}\mathrm{Zr}$ at $27A$ MeV [61] with statistical calculations including model prescriptions of Bortignon *et al.* [47] (solid line), Smerzi *et al.* [51] (dot-dashed line) and Chomaz [50] (dotted line). Bottom: same spectrum compared with the prediction of a statistical calculation including a width increasing with E^* according to eq. (6) shown as a dashed line.

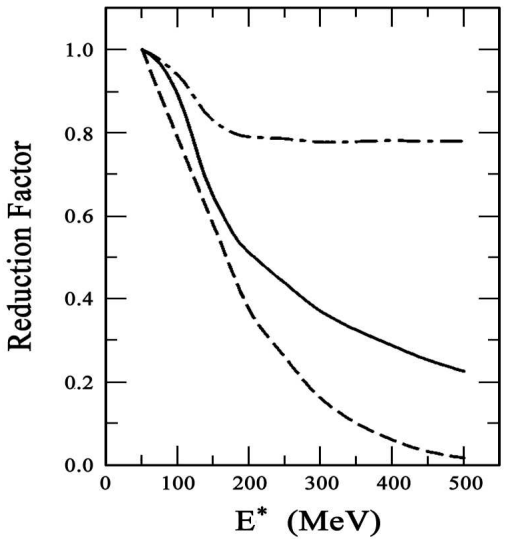

Fig. 17. Predictions for the GDR quenching factor as a function of E^* [61] according to the models of Bortignon *et al.* [47] (solid line), Smerzi *et al.* [51] (dot-dashed line) and Chomaz [50] (dashed line).

The effect of the increasing width on the spectral shape can be evaluated in fig. 14 where the experimental integrated yield in the regions 12–20 MeV and 20–35 MeV are compared to the predictions of a statistical calculation including the parametrization given by eq. (6) (shown as a dashed line). As a reference, the yield according to the standard statistical calculation is also reported in the same figure as a solid line. The figure unambiguously shows that, while in the GDR peak region the calculation with an increasing width lies slightly above the data, this is no longer the case in the region 20–35 MeV where it predicts an increase even larger than the standard statistical calculation. Similar consideration holds for the slope of the spectrum calculated above 20 MeV after bremsstrahlung subtraction [61]. The reasons can be found in the statistical dipole emission rate formula (eq. (4)) where two ingredients contribute to the observed effect. The first is the level density ratio which is roughly proportional to $\exp(-E_\gamma/T)$ and with increasing temperature tends to increase the γ multiplicity at higher energies by decreasing the slope of the spectrum. The second is the factor E_γ^2 which multiplies the Lorentzian representing the GDR strength function. It shifts the γ yield to higher energies when the GDR width increases. Therefore, the overall effect, as already observed, is to induce a shift in the yield rather then a quenching and this is not observed in the data. Such considerations hold for all models including a width increase in the calculation. The important conclusion of the work is that the GDR gamma-ray saturation is consistent with a disappearance of the GDR strength above E^* about 250 MeV. This led the authors to conclude that $E^*/A \sim 2.5$ MeV represents a limit for the existence of the dipole vibration for $A \sim 110$ nuclei [44].

Similar considerations hold also for $37A$ MeV data even if a slightly lower gamma multiplicity was observed. The comparison of the average multiplicity measured in the 27 and $37A$ MeV reactions with RIKEN data which were extracted in the same region of E^* but at lower beam energies indicates a significant decrease of the γ yield with bombarding energy suggesting the existence of a dynamical effect which could influence the equilibration time of the hot source and the development of collective motion [45]. However, a different pre-equilibrium emission among the reactions, not always properly evaluated, could lead to emitting sources with different average masses and charges, therefore affecting the emission probability which depends on $N \cdot Z/A$ of the emitting system. Besides, the comparison of the gamma yield between experiments performed using different experimental setups can be biased by the different response function of the detectors. These considerations may weaken the conclusion of a dependence of the γ-ray yield on beam energy.

A few other elements of this complicated puzzle remain still unexplained. In particular, the mechanism that suppresses the collective motion at high excitation energies is still unclear as well as the exact energy region where the quenching appears. In fact, in the GANIL experiments, all the systems were populated at excitation energies above the cut-off energy of 250 MeV, precluding a detailed study of the onset of the quenching. Besides, the introduction of

a sharp cutoff approximation to reproduce the data, while pointing to a sudden disappearance of the GDR gamma emission does not preclude the existence of a progressive quenching of the GDR yield already below 300 MeV excitation energy which is actually predicted by different models (see fig. 17).

It thus appeared important to investigate a region of lower excitation energies where the saturation of the yield was expected to set in and to map the progressive disappearance of the GDR. The experiment performed at the LNS-Catania with MEDEA coupled to Superconductive Solenoid SOLE which focused the evaporation residues on the focal plane MACISTE [62] investigated the excitation energy region between 160 and 290 MeV through the study of the reactions ^{116}Sn + ^{12}C at 17 and 23A MeV and ^{116}Sn + ^{24}Mg at 17A MeV. The choice of reactions with a strong mass asymmetry was driven by the need to reduce the spread in momentum transfer which leads to a better determination of the excitation energy of the system. The reverse kinematics were used to better match the SOLE acceptance. A single velocity window centered around the center-of-mass velocity was selected for each reaction and gamma-ray spectra were built accordingly. The spectra were compared to standard statistical calculations assuming a fixed width Γ = 12 MeV, 100% of EWSR and a centroid energy $E_{GDR} = 76/A^{1/3}$ similarly to what was previously done for the reactions at 27 and 37A MeV.

The results shown in fig. 18 indicate that while the spectra up to E^* = 200 MeV are remarkably well reproduced by the calculation over almost six order of magnitude this is no longer the case for the spectrum at E^* = 290 MeV where the calculation slightly overshoots the data. In the same figure two spectra from the reaction at 37A MeV measured at E^* = 350 and 430 MeV are shown as a comparison together with the corresponding calculations. The overall set of data shows a clear evolution of the GDR yield with E^* from the low excitation energy domain where the statistical scenario provides a good description of the data to a region of excitation energies exceeding 300 MeV where the GDR quenching becomes progressively more pronounced suggesting that the critical region for the onset of the GDR quenching is between 200 and 290 MeV in nuclei of mass $A \sim$ 110–130. All evidence collected points to a limiting excitation energy of about 250 MeV for the existence of collective motion which corresponds to a limiting $E^*/A \sim$ 2.5 MeV. Above such a value a rather strong suppression of the GDR gamma emission is observed. This effect cannot be explained by a continuous increase of the width. The reason of the suppression has to be found in the competition between the development of collective motion and particle decay.

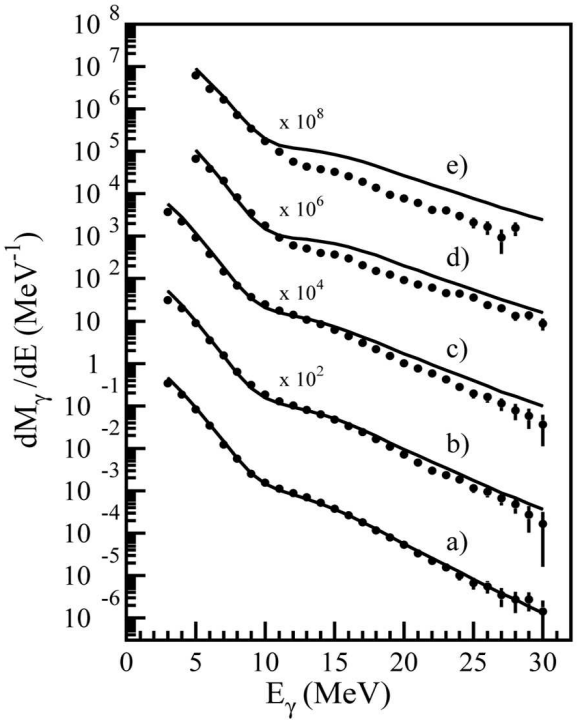

Fig. 18. Gamma-ray spectra measured at 160, 200, 290, 350 and 430 MeV excitation energy (a-e) in coincidence with evaporation residues. The spectra at E^* = 160 and 200 MeV are from the reactions ^{116}Sn + ^{12}C at 17 and 23A MeV, the one at E^* = 290 MeV is from the reaction ^{116}Sn + ^{24}Mg at 17A MeV while the spectra at higher excitation energies were measured in the reaction ^{36}Ar + ^{98}Mo at 37A MeV. Solid lines represent the corresponding CASCADE calculations performed assuming 100% of the EWSR and a constant width Γ = 12 MeV.

6.4 Hot GDR disappearance in nuclei of mass A ∼ 60–70

Since Giant Dipole Resonances are a general feature of all nuclei it is important to investigate other mass regions to study the evolution of their main features. In the following, we will concentrate on the high-temperature region where further evidence for a saturation of the γ yield was recently observed in the mass region $A \sim$ 60–70. The first information concerning the features of the GDR built on the ground state were collected in the early seventies, as in the case of the mass $A \sim$ 120, through photo-neutron reaction studies [6].

The properties of the GDR built on excited states were then investigated in detail through the study of ^{59,63}Cu nuclei [63,64]. Different entrance channels and excitation energies were investigated in order to disentangle the effects driven by spin and temperature on the width and the energy of the resonance [63,64]. The collected systematics up to E^* = 100 MeV shows a centroid energy remarkably stable with temperature while the width increases from about 6–7 MeV in the ground state, depending on the isotope, up to about 15 MeV [1,63,64].

More recently the study of the reactions ^{40}Ca + ^{48}Ca and ^{40}Ca + ^{46}Ti at 25A MeV performed at the LNS-Catania with the TRASMA detector [65] demonstrated the existence of a limiting temperature for the collective motion in systems of mass $A \sim$ 60 [66,67]. In this experiment pre-equilibrium γ-rays were also investigated [67] and a detailed description of this topic can be found in refs. [68–72]. Heavy residues populated at about E^* =

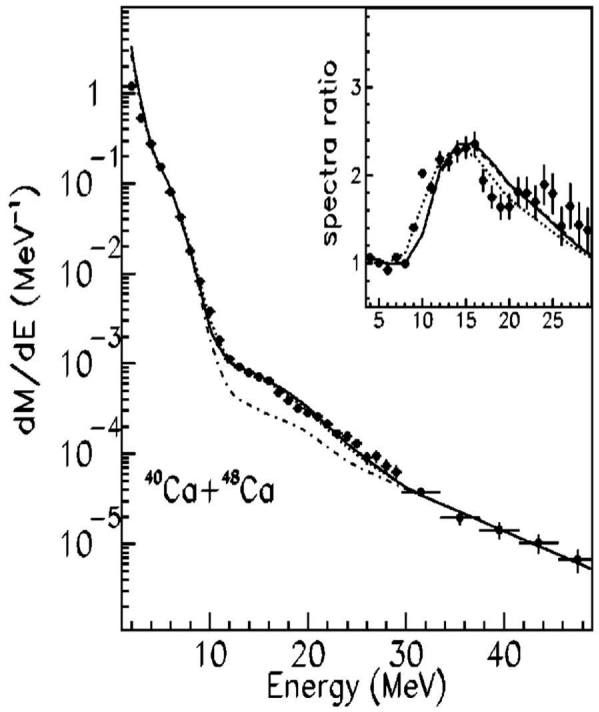

Fig. 19. Gamma-ray spectrum measured in the reaction $^{40}\mathrm{Ca} + {}^{48}\mathrm{Ca}$ at $25A$ MeV in coincidence with evaporation residues. The full line is a calculation assuming a cut-off energy for the GDR emission at $E^* = 260$ MeV and a width $\Gamma = 15$ MeV. The dashed line is a calculation assuming a smooth cut-off expression according to [47]. The dotted line is instead obtained assuming again a cut-off energy at $E^* = 260$ MeV but a mass $A = 70$ for the emitting system. The dot-dashed line is a GDR zero strength calculation used to linearize the experimental data and calculations shown in the inset.

330–350 MeV were detected in coincidence with gamma-rays whose spectra were compared to statistical calculations assuming a centroid energy $E_{GDR} = 16.8$ MeV, 100% of EWSR and a width $\Gamma = 15$ MeV kept constant all along the decay process. The comparison provided evidence for a quenching of the yield similarly to what was previously observed in the mass region $A \sim 120$. In order to reproduce the data on ^{48}Ca the authors introduced a sharp suppression of the GDR gamma emission above $E^* = 260$ MeV corresponding to a $E_{cut\text{-}off}/A \simeq 4.7A$ MeV [66,67]. The statistical calculation shown as a solid line in fig. 19 nicely reproduced the whole spectrum. A smaller value for the cut-off energy was needed in the case of the ^{46}Ti target. The authors also investigated the effect on the cut-off of including a width dependent on excitation energy. A width increasing up to the saturation value of 15 MeV reached at $E^* = 100$ MeV, was used in the calculation and a cut-off energy of 240 MeV was extracted [67].

More refined calculations including the prescriptions of different smooth cut-offs were also performed. A good description of the data was obtained for both reactions adopting the smooth cut-off suggested by Bortignon *et al.* [47] which led to a slightly higher values of the cut-off energy compared to the sharp cut-off approximation. In particular, assuming a cut-off energy corresponding to $\Gamma^{\downarrow}/(\Gamma^{\downarrow} + \Gamma_{ev}) = 1/2$, values of about $5.4 \pm 0.5A$ MeV and $4.7 \pm 0.9A$ MeV were extracted for ^{48}Ca and ^{46}Ti targets. Figure 19 includes as a dashed line the statistical calculation performed using the smooth cut-off expression of ref. [47]. No difference with the calculation using a sharp cut-off approximation can be observed. Other prescriptions were investigated including the one assuming a width continuously increasing with excitation energy but a poorer agreement with data was found [67] confirming the results previously observed in the mass region $A \sim 110$–130. The important conclusion of this work concerns the first evidence for a limiting excitation energy for the GDR excitation in $A \sim 60$–70 nuclei. Its value of about 5 MeV/nucleon differs significantly from the one measured for nuclei in the mass region $A \sim 110$–130 and suggests the existence of a mass dependence of the limiting temperature for the excitation of collective motion.

7 Mass dependence of the limiting temperature

The study of the liquid-gas phase transition in nuclear matter represents an issue widely investigated during the last few years. It has been proposed that the presence of collective states can be a signature of the existence of a compound nucleus and that the disappearance of the GDR could be a further evidence for a phase transition in nuclei [49,73]. In particular, the GDR disappearance at high excitation energies gives access to the maximum excitation energy at which nuclei can still show a collective behavior. This energy can give complementary information to the caloric-curve studies which provide important information concerning the existence of a liquid-gas phase transition. Recently, the analysis of the nuclear caloric curve for nuclei in different mass regions has shown evidence for the existence of a plateau at high excitation energies which represents the region of the equilibrium phase coexistence between liquid and vapor. The limiting temperature represented by the plateau has been observed to decrease as a function of the nuclear mass [15]. This affects the excitation energy value at which the plateau appears which decreases with mass as shown in fig. 20 [15].

Interesting similarities with this trend were found studying the limiting excitation energy for the collective motion. In fact, the results indicate a decrease of the maximum excitation energy for the collective motion from about 5 MeV/nucleon for nuclei of mass $A \sim 60$–70 to about 2.5 MeV/nucleon for nuclei in the mass region $A \sim 110$. Moreover, the values of the excitation energies extracted in both mass regions are close to the energies where the plateau of the caloric curve appears (see fig. 20). This intriguing feature suggests the possible occurrence of a transition from order to chaos in nuclei for excitation energies close to the values where signals of a liquid-gas

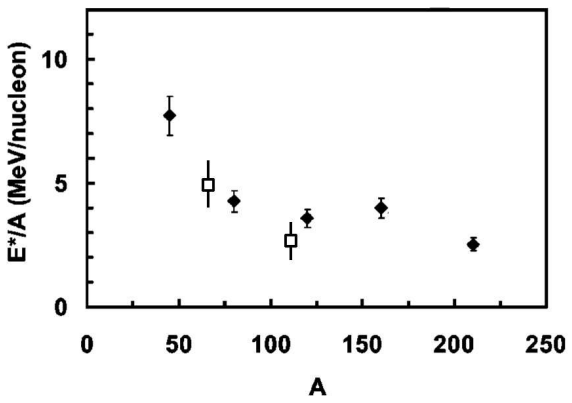

Fig. 20. Excitation energy per nucleon at which the limiting temperature is reached as a function of the system mass [15]. Open symbols are the limiting excitation energies per nucleon for the collective motion extracted in two mass regions.

phase transition were claimed to be present. The link between the two observations deserves further investigations.

8 Conclusions and perspectives

In the last twenty years of investigation, the main properties of the GDR built on excited states have been measured and understood. The most complete systematics was studied for medium mass nuclei around $A \sim 110$–120 for which measurements were performed for excitation energies between 10 and 500 MeV and spins up to $J \sim 60\hbar$ through both fusion reactions and inelastic scattering yielding an extraordinarily detailed picture of the GDR behavior.

No significant shift of the centroid energy with either temperature or angular momentum has been observed. The width increases both with excitation energy and spin, the latter becoming important only above about $35\hbar$. Inelastic-scattering experiments which populate a range of excitation energies at low spin and fusion experiments using a spin spectrometer setup have led to an experimental de-convolution of temperature and spin effects. It is now well established that the GDR width increases with spin up to $J \sim 60\hbar$ and with temperature up to at least $T \sim 3$ MeV. This behavior is satisfactorily accounted for by the adiabatic thermal fluctuation model.

Above these values many claims for saturation of the GDR width have been made in the literature. However above $60\hbar$ fission sets in as the main decay channel and increasing the angular momentum in the entrance channel does not probe higher spins. Many recent experiments have succeeded to reach temperatures above $T \sim 3$ MeV. In this region a saturation of the GDR gamma-ray yield is observed while statistical calculations predict a continuous increase with excitation energy. The results can be reproduced by a surprisingly sudden drop of the GDR strength at $E^* \sim 250$ MeV. The spectra are not compatible with a continuous increase of the width as was predicted in several theoretical papers. Nonetheless, it cannot be concluded that the width saturates since, once the strength has vanished, the characteristics of the GDR are no longer probed. The drop in strength is related to a competition between equilibration of collective motion and particle decay. Several models were developed to account for such effects and all predict a reduction of the gamma emission probability, albeit with different laws. The lack of data in the critical excitation energy region precludes us today from distinguishing between the different models.

Measurements for lighter nuclei at high excitation energies show the same trends but the limiting excitation energy for the existence of the GDR is $E^*_{lim}/A = 5$ MeV compared to approximately 2.5 MeV in the $A \sim 110$ mass region. It is intriguing to compare these values with the limiting excitation energies extracted from caloric-curve studies. A link between the disappearance of collective motion and a liquid-gas phase transition appears as a distinct possibility worthy of further studies.

Despite the global understanding of the characteristics of collective motion at high temperatures achieved over the past years several issues must still be elucidated. In particular, it would be of great interest to assess the sharpness of the disappearance of the GDR by measuring a more complete excitation function in this region. A slight bombarding-energy dependence of the GDR yield at a given excitation energy has been observed and remained hitherto unexplained. This effect, probably of dynamical nature, needs to be confirmed experimentally and understood theoretically. Finally, the link between the disappearance of the GDR and phase transition may be better understood by extending the systematics of high-energy GDR studies to heavier systems as, *e.g.*, in the lead region.

We would like to thank Drs P. Piattelli, P. Sapienza, R. Coniglione, R. Alba for many helpful discussions and valuable contributions in proofreading the manuscript. We would also thank all the participants in the MEDEA experiments at GANIL and LNS-Catania.

References

1. K.A. Snover, Annu. Rev. Nucl. Part. Sci. **36**, 545 (1986).
2. J.J. Gaardhøje, Annu. Rev. Nucl. Part. Sci. **42**, 483 (1992).
3. G.C. Baldwin, G.S. Klaiber, Phys. Rev. **71**, 3 (1947).
4. G.C. Baldwin, G.S. Klaiber, Phys. Rev. **73**, 1156 (1948).
5. M. Goldhaber, E. Teller, Phys. Rev. **74**, 1046 (1948).
6. B.L. Berman, S.C. Fultz, Rev. Mod. Phys. **47**, 713 (1975).
7. H. Steinwedel, J.H.D. Jensen, Z. Naturforsch A **5**, 413 (1950).
8. D.M. Brink, PhD Thesis, University of Oxford (1955).
9. F.S. Dietrich, J.C. Browne, W.J. O'Connell, M.J. Kay, Phys. Rev. C **10**, 795 (1974).
10. M.A. Kovash, S.L. Blatt, R.N. Boyd, T.R. Donoghue, H.J. Hausmann, A.D. Bacher, Phys. Rev. Lett. **42**, 700 (1979).
11. D.H. Dowell, G. Feldman, K.A. Snover, A.M. Sandorfi, M.T. Collins, Phys. Rev. Lett. **50**, 1191 (1983).
12. J.O. Newton, B. Herskind, R.M. Diamond, E.L. Dines, J.E. Draper, K.H. Lindenberger, C. Schück, S. Shih, F.S. Stephens, Phys. Rev. Lett. **46**, 1383 (1981).

13. F. Pühlhofer, Nucl. Phys. A **280**, 267 (1977).
14. A. Bohr, B.R. Mottelson, *Nuclear Structure*, Vol. **1** (Benjamin Inc., London, 1969).
15. J.B. Natowitz, R. Wada, K. Hagel, T. Keutgen, M. Murray, A. Makeev, L. Qin, P. Smith, C. Hamilton, Phys. Rev. C **65**, 034618 (2002) and references therein.
16. M. Gallardo, M. Diebel, T. Døssing, R.A. Broglia, Nucl. Phys. A **443**, 415 (1985).
17. J.M. Pacheco, C. Yannouleas, R.A. Broglia, Phys. Rev. Lett. **61**, 294 (1988).
18. Y. Alhassid, B. Bush, S. Levit, Phys. Rev. Lett. **71**, 1926 (1988).
19. D. Kusnezov, Y. Alhassid, K.A. Snover, Phys. Rev. Lett. **81**, 542 (1998) and references therein.
20. P. Heckman, D. Bazin, J.R. Beene, Y. Blumenfeld, M.J. Chromik, M.L. Halbert, J.F. Liang, E. Mohrmann, T. Nakamura, A. Navin, B.M. Sherrill, K.A. Snover, M. Thoennessen, E. Tryggestad, R.L. Varner, Phys. Lett. B **555**, 43 (2003).
21. M. Thoennessen, Nucl. Phys. A **731**, 131 (2004) and references therein.
22. F. Camera, A. Bracco, V. Nanal, M.P. Carpenter, F. Della Vedova, S. Leoni, B. Million, S. Mantovani, M. Pignanelli, O. Wieland, B.B. Back, A.M. Heinz, R.V.F. Janssens, D. Jenkins, T.L. Khoo, F.G. Kondev, T. Lauritsen, C.J. Lister, B. McClintock, S. Mitsuoka, E.F. Moore, D. Seweryniak, R.H. Siemssen, R.J. Van Swol, D. Hofmann, M. Thoennessen, K. Eisenman, P. Heckman, J. Seitz, R. Varner, M. Halbert, I. Dioszegi, A. Lopez-Martens, Phys. Lett. B **560**, 155 (2003).
23. J.J. Gaardhøje, C. Ellegaard, B. Herskind, S.G. Steadman, Phys. Rev. Lett. **53**, 148 (1984).
24. J.J. Gaardhøje, C. Ellegaard, B. Herskind, R.M. Diamond, M.A. Delaplanque, G. Dines, A.O. Macchiavelli, F.S. Stephens, Phys. Rev. Lett. **56**, 1783 (1986).
25. D.R. Chakrabarty, S. Sen, M. Thoennessen, N. Alamanos, P. Paul, R. Schicker, J. Stachel, J.J. Gaardhøje, Phys. Rev. C **36**, 1886 (1987).
26. A. Bracco, J.J. Gaardhøje, A.M. Bruce, J.D. Garrett, B. Herskind, M. Pignanelli, D. Barnéoud, H. Nifenecker, J.A. Pinston, C. Ristori, F. Schussler, J. Bacelar, H. Hofmann, Phys. Rev. Lett. **62**, 2080 (1989).
27. G. Enders, F.D. Berg, K. Hagel, W. Kühn, V. Metag, R. Novotny, M. Pfeiffer, O. Schwalb, R.J. Charity, A. Gobbi, R. Freifelder, W. Henning, K.D. Hildenbrand, R. Holzmann, R.S. Mayer, R.S. Simon, J.P. Wessels, G. Casini, A. Olmi, A.A. Stefanini, Phys. Rev. Lett. **69**, 249 (1992).
28. H.J. Hofmann, J.C. Bacelar, M.N. Harakeh, T.D. Poelhekken, A. van der Woude, Nucl. Phys. A **571**, 301 (1994).
29. E. Ramakrishnan, T. Baumann, A. Azhari, R.A. Kryger, R. Pfaff, M. Thoennessen, S. Yokoyama, J.R. Beene, M.L. Halbert, P.E. Mueller, D.W. Stracener, R.L. Varner, R.J. Charity, J.F. Dempsey, D.G. Sarantites, L.G. Sobotka, Phys. Rev. Lett. **76**, 2025 (1996).
30. M. Mattiuzzi, A. Bracco, F. Camera, W.E. Ormand, J.J. Gaardhøje, A. Maj, B. Million, M. Pignanelli, T. Tveter, Nucl. Phys. A **612**, 262 (1997).
31. A. Bracco, F. Camera, M. Mattiuzzi, B. Million, M. Pignanelli, J.J. Gaardhøje, A. Maj, T. Ramsøy, T. Tveter, Z. Zelazny, Phys. Rev. Lett. **74**, 3748 (1995).
32. W.E. Ormand, P.F. Bortignon, R.A. Broglia, Nucl. Phys. A **599**, 57c (1996).
33. G. Gervais, M. Thoennessen, W.E. Ormand, Nucl. Phys. A **649**, 173c (1999).
34. W.E. Ormand, Nucl. Phys. A **649**, 145c (1999).
35. P. Chomaz, Phys. Lett. B **347**, 1 (1995).
36. S.K. Rathi, D.R. Chakrabarty, V.M. Datar, Suresh Kumar, E.T. Mirgule, A. Mitra, V. Nanal, H.H. Oza, Phys. Rev. C **67**, 024603 (2003).
37. M.P. Kelly, J.F. Liang, A.A. Sonzogni, K.A. Snover, J.P.S. van Schagen, J.P. Lestone, Phys. Rev. C **56**, 3201 (1997).
38. M.P. Kelly, K.A. Snover, J.P.S. van Schagen, M. Kicińska-Habior, Z. Trznadel, Phys. Rev. Lett. **82**, 3404 (1999).
39. K.A. Snover, Nucl. Phys. A **687**, 337c (2001).
40. O. Wieland, S. Barlini, V.L. Kravchuk, F. Camera, F. Gramegna, A. Maj, G. Benzoni, N. Blasi, S. Brambilla, M. Brekiesz, M. Bruno, G. Casini, M. Chiari, E. Geraci, A. Giussani, M. Kmiecik, S. Leoni, A. Lanchais, P. Mastinu, B. Million, A. Moroni, A. Nannini, A. Ordine, G. Vannini, L. Vannucci, J. Phys. G: Nucl. Part. Phys. **31**, S1973 (2005).
41. H. Nifenecker, J. Blachot, J. Crançon, A. Gizon, A. Lleres, Nucl. Phys. A **447**, 533c (1985).
42. J.J. Gaardhøje, A.M. Bruce, J.D. Garrett, B. Herskind, D. Barnéoud, M. Maurel, H. Nifenecker, J.A. Pinston, P. Perrin, C. Ristori, F. Schussler, A. Bracco, M. Pignanelli, Phys. Rev. Lett. **59**, 1409 (1987).
43. K. Yoshida, J. Kasagi, H. Hama, M. Sakurai, M. Kodama, K. Furutaka, K. Ieki, W. Galster, T. Kubo, M. Ishihara, Phys. Lett. B **245**, 7 (1990).
44. J.H. Le Faou, T. Suomijärvi, Y. Blumenfeld, P. Piattelli, C. Agodi, N. Alamanos, R. Alba, F. Auger, G. Bellia, Ph. Chomaz, R. Coniglione, A. Del Zoppo, P. Finocchiaro, N. Frascaria, J.J. Gaardhøje, J.P. Garron, A. Gillibert, M. Lamehi-Racti, R. Liguori-Neto, C. Maiolino, E. Migneco, G. Russo, J.C. Roynette, D. Santonocito, P. Sapienza, J.A. Scarpaci, A. Smerzi, Phys. Rev. Lett. **72**, 3321 (1994).
45. P. Piattelli, T. Suomijärvi, Y. Blumenfeld, D. Santonocito, C. Agodi, N. Alamanos, R. Alba, F. Auger, G. Bellia, Ph. Chomaz, M. Colonna, R. Coniglione, A. Del Zoppo, P. Finocchiaro, N. Frascaria, A. Gillibert, J.H. Le Faou, K. Loukachine, C. Maiolino, E. Migneco, J.C. Roynette, P. Sapienza, J.A. Scarpaci, Nucl. Phys. A **649**, 181c (1999).
46. D.M. Brink, Nucl. Phys. A **519**, 3c (1990).
47. P.F. Bortignon, A. Bracco, D. Brink, R.A. Broglia, Phys. Rev. Lett. **67**, 3360 (1991).
48. P. Donati, N. Giovanardi, P.F. Bortignon, R.A. Broglia, Phys. Lett. B **383**, 15 (1996).
49. P. Chomaz, M. Di Toro, A. Smerzi, Nucl. Phys. A **563**, 509 (1993).
50. P. Chomaz, Nucl. Phys. A **569**, 203c (1994).
51. A. Smerzi, A. Bonasera, M. Di Toro, Phys. Rev. C **44**, 1713 (1991).
52. A. Smerzi, M. Di Toro, D.M. Brink, Phys. Lett. B **320**, 216 (1994).
53. A. Bonasera, M. Di Toro, A. Smerzi, D.M. Brink, Nucl. Phys. A **569**, 215c (1994).
54. R.A. Broglia, P.F. Bortignon, A. Bracco, Prog. Part. Nucl. Phys. **28**, 517 (1992).
55. K. Yoshida, J. Kasagi, H. Hama, M. Sakurai, M. Kodama, K. Furutaka, K. Ieki, W. Galster, T. Kubo, M. Ishihara, A. Galonsky, Phys. Rev. C **46**, 961 (1992).
56. J. Kasagi, K. Yoshida, Nucl. Phys. A **557**, 221c (1993).
57. J. Kasagi, K. Yoshida, Nucl. Phys. A **569**, 195c (1994).

58. E. Migneco, C. Agodi, R. Alba, G. Bellia, R. Coniglione, A. Del Zoppo, P. Finocchiaro, C. Maiolino, P. Piattelli, G. Raia, P. Sapienza, Nucl. Instrum. Methods Phys. Res. A **314**, 31 (1992).
59. D. Santonocito, P. Piattelli, Y. Blumenfeld, T. Suomijärvi, C. Agodi, N. Alamanos, R. Alba, F. Auger, G. Bellia, Ph. Chomaz, M. Colonna, R. Coniglione, A. Del Zoppo, P. Finocchiaro, N. Frascaria, A. Gillibert, J.H. Le Faou, K. Loukachine, C. Maiolino, E. Migneco, J.C. Roynette, P. Sapienza, J.A. Scarpaci, Phys. Rev. C **66**, 044619 (2002).
60. W.E. Ormand, P.F. Bortignon, A. Bracco, R.A. Broglia, Phys. Rev. C **40**, 1510 (1989).
61. T. Suomijärvi, Y. Blumenfeld, P. Piattelli, J.H. Le Faou, C. Agodi, N. Alamanos, R. Alba, F. Auger, G. Bellia, Ph. Chomaz, R. Coniglione, A. Del Zoppo, P. Finocchiaro, N. Frascaria, J.J. Gaardhøje, J.P. Garron, A. Gillibert, M. Lamehi-Racti, R. Liguori-Neto, C. Maiolino, E. Migneco, G. Russo, J.C. Roynette, D. Santonocito, P. Sapienza, J.A. Scarpaci, A. Smerzi, Phys. Rev. C **53**, 2258 (1996).
62. G. Bellia, P. Finocchiaro, K. Loukachine, C. Agodi, R. Alba, L. Calabretta, R. Coniglione, A. Del Zoppo, C. Maiolino, E. Migneco, P. Piattelli, G. Raciti, D. Rifuggiato, D. Santonocito, P. Sapienza, IEEE Trans. Nucl. Sci. **43**, 1737 (1996).
63. M. Kicińska-Habior, K.A. Snover, C.A. Gossett, J.A. Behr, G. Feldman, H.K. Glatzel, J.H. Gundlach, E.F. Garman, Phys. Rev. C **36**, 612 (1987).
64. B. Fornal, F. Gramegna, G. Prete, R. Burch, G. D'Erasmo, E.M. Fiore, L. Fiore, A. Pantaleo, V. Paticchio, G. Viesti, P. Blasi, N. Gelli, F. Lucarelli, M. Anghinolfi, P. Corvisiero, M. Taiuti, A. Zucchiatti, P.F. Bortignon, D. Fabris, G. Nebbia, J.A. Ruiz, M. Gonin, J.B. Natowitz, Z. Phys. A **340**, 59 (1991).
65. A. Musumarra, G. Cardella, A. Di Pietro, S.L. Li, M. Papa, G. Pappalardo, F. Rizzo, S. Tudisco, J.P.S. van Schagen, Nucl. Instrum. Methods A **370**, 558 (1996).
66. S. Tudisco, G. Cardella, F. Amorini, A. Anzalone, A. Di Pietro, P. Figuera, F. Giustolisi, G. Lanzalone, Lu Jun, A. Musumarra, M. Papa, S. Pirrone, F. Rizzo, Europhys. Lett. **58**, 811 (2002).
67. F. Amorini, G. Cardella, A. Di Pietro, P. Figuera, G. Lanzalone, Lu Jun, A. Musumarra, M. Papa, S. Pirrone, F. Rizzo, W. Tian, S. Tudisco, Phys. Rev. C **69**, 014608 (2004).
68. M. Papa, contributed paper to the *WCI Texas A&M Conference, College Station, USA, 2005.*
69. M. Papa, A. Bonanno, F. Amorini, A. Bonasera, G. Cardella, A. Di Pietro, P. Figuera, T. Maruyama, G. Pappalardo, F. Rizzo, S. Tudisco, Phys. Rev. C **68**, 034606 (2003).
70. M. Papa, W. Tian, G. Giuliani, F. Amorini, G. Cardella, A. Di Pietro, P. Figuera, G. Lanzalone, S. Pirrone, F. Rizzo, D. Santonocito, Phys. Rev. C **72**, 064608 (2005).
71. D. Pierroutsakou, M. Di Toro, F. Amorini, V. Baran, A. Boiano, A. De Rosa, A. D'Onofrio, G. Inglima, M. La Commara, A. Ordine, N. Pellegriti, F. Rizzo, V. Roca, M. Romoli, M. Sandoli, M. Trotta, S. Tudisco, Eur. Phys. J. A **16**, 423 (2003).
72. D. Pierroutsakou, A. Boiano, A. De Rosa, M. Di Pietro, G. Inglima, M. La Commara, Ruhan Ming, B. Martin, R. Mordente, A. Ordine, F. Rizzo, V. Roca, M. Romoli, M. Sandoli, F. Soramel, L. Stroe, M. Trotta, E. Vardaci, Eur. Phys. J. A **17**, 71 (2003).
73. A. Bonasera, M. Bruno, P.F. Mastinu, C.A. Dorso, Riv. Nuovo Cimento **23**, no. 2 (2000).